Dear editor,

We thank both of the reviewers for their comments. Both reviewers are highly supportive of publication of this manuscript.

Importantly, none of their comments represented substantial criticism to any of our interpretations. All of their suggestions represented corrections or suggestions for the presentation of the paper. We incorporated almost all of them and motivate the few exceptions where we respectfully chose otherwise in the below reply letter. We therefore hope this version of the manuscript can be accepted for publication.

Sincerely, on behalf of all authors,

Appy Sluijs

Anonymous Reviewer #1

Sluijs et al. used the previously analyzed samples which were stored for over a decade. As I am interested in GDGTs, I was curious how the old and new GDGT data would differ, although I assume the offset would be small if stored properly and measured in good condition of the HPLC/MS. Figure 3 shows the result and regression analysis between the old and measured GDGTs results. Both TEX86 and BIT look comparable. However, I found that there are few outliers in the TEX86 dataset from the supplementary data. I plotted all their new vs old TEX86, and the Rˆ2 value is lower to 0.66. Still comparable statistically, however, the authors did not mention about the outliers.

REPLY: These outliers represent data points for which the intensity of some isomers was insufficient in our reruns for proper quantification. For these 5 samples, TEX86 values were anomalously low as a consequence. These were the open fields in the spread sheet of the raw data but for clarity we have now marked them 'below detection' for the revised version of the manuscript. This further clarifies based on which data the 0.82 R^2 of Figure 3 is based.

I appreciate the authors for providing their valuable dataset and kindly included the spreadsheet calculation for the readers to follow. For RI (ring index), however, I found that the calculations were all missing while it can be calculated from the dataset. I calculated again from their data but the values were slightly different. The maximum difference between the reported value (column BX) and the calculation I did is up to 0.11 RI unit. Although the difference is small, this would impact on some of the samples that have _RI near 0.3, screening whether the data is reliable or unreliable near its cutoff value.

REPLY: We thank the reviewer very much for noticing this. The discrepancy was caused by an error in our excel calculations so that Cren isomer was not properly included. The numbers have been corrected in the revised supplement and Figure 5. The difference is indeed minor as the reviewer indicates and in fact it results in lower ΔRI and so we found no extra unreliable data points in our rescreening of the data.

Overall, I suggest a moderate revision of the manuscript, especially in the data analysis first, before it can be accepted by CP. Also, the manuscript contained plagiarism (line 160-163) and many run-on sentences which made it difficult in absorbing the information when reading, therefore, I suggest a more improvement in the scientific writing for the next version.

REPLY: We have carefully reconsidered the text, and reworded sections that may have been unclear.

Some specific comments are below:

Line 20-21: add "ACEX"

REPLY: this has been done

Line 20-52: the abstract seems to be too long and includes too much information of the study results in detail. Also, line 46-50 is just copied and pasted here from the main text (line 806-810).

REPLY: we have shortened the abstract significantly and avoided textual overlap with the rest of the text.

Line 37: the background SSTs in early Eocene generally exceed

REPLY: this has been done

Line 71-77: run-on sentence: divided into two sentences
REPLY: this has been done

Line 77-84: I understand citing all the references to supplement, however, 17 citations are too overloaded in one sentence for the reader. I suggest organizing the citation to where they would belong. For example, link and cite Pagani et al. (2006) with “molecular fossils” which examined the _D of n-alkane addressing the hydrologic cycle. Or breakdown the sentence and cite only the important references.
REPLY: we have cited three of the early papers that showed the potential for follow-up work.

Line 160-163: this sentence should be rephrased. It is exactly the same as written in Hollis et al. (2019) describing the BAYSPAR, but one word added here (plagiarism).
REPLY: this has been done

Line 169: add the TEX86 value range of which converted SSTs differs between linear & non-linear
REPLY: This has been extensively discussed in the literature and it seems that the divergence occurs close to the maximum value in the calibration dataset (ca. 0.70), which we have included now.

Line 190-191: I suggest to remove “based on high BIT index value” and add the range of BIT results from the study after the equation.
REPLY: this has been done and we have added a sentence reporting on a previous subjectively defined threshold assigned on the study section (Sluijs et al., 2009).

Line 207: specify the GDGT. If just GDGT, does it mean both iso- and brGDGts?
REPLY: this has been specified to isoGDGTs

Line 219-224: add the depth range of the deep contribution (Talyor et al., 2013) and also the reconstructed water depth of Site M00004A, meaning shallower shelf environ- ment, to connect the interpretation of negligible deep source.
REPLY: This has been done (>1000 m)

Line 233: use “[Crenarchaeol isomer]” for consistent compound name in all equations. this also implies for the names throughout the paper.
REPLY: this has been done

Line 234: “significant presence (or contribution) of anaerobic methanotrophy”
REPLY: this has been done

Line 242-243: provide references
REPLY: this has been done

Line 251: “Crenarchaeol isomer” for consistency of the compound name throughout the paper.
REPLY: this has been done

Line 299: I would rather suggest starting with ‘brGMGTs’ and supplement that this was previously reported as H-shaped brGDGTs, since the former is the major compound referred throughout the manuscript. Also, I suggest removing any description of ‘Hshape brGDGTs’ afterwards, as it makes it more confusing.
REPLY: This suggestion has been followed

Line 344: the precision of TEX86 unit or converted SSTs unit?
REPLY: We now explain that this regards the uncertainty calculated to the SST domain.

Line 351-353: same comment with line 344. In addition, I am confused with what “both” labs means.
REPLY: We have deleted this confusing sentence.

Line 409: interval should be between 371.0 to “369.0” mcd, based on Figure 4 and Sluijs et al. (2009),
REPLY: Indeed, thank you for noticing. We have changed this accordingly.

Line 416-417: add the linear regression line in Figure 4 and supplement what “explaining 26 % of the variation” means
REPLY: This has been done and the statement on variation has been clarified; this number is taken directly from the R^2 (0.26) of the linear regression.

Line 428: I suggest to cite “Figure 6” in the first sentence, so the reader can easily compare the visualized data with the text, starting from the beginning of section or paragraph.
REPLY: this has been done

Line 442-452: Rather than directly moving on to the discussion of the method and result, I suggest to add a brief explanation of what lignite is and why lignite was used as the representative of terrestrial source for the readers to easily understand the concept.
REPLY: This has been done. We use the peat and lignite databases because they represent comprehensive datasets and therefore allow a rough calculation of the potential isoGDGT contribution.

Line 445: supplement how the absolute concentration is calculated (e.g. what standard used).
REPLY: Absolute concentration was incorrect. It has been changed to raw signal intensity.

Line 467: “GDGT-2 and -3”. Suggest describing the compounds be consistent throughout the paper.
REPLY: this has been done

Line 473-478: This is true based on the isoGDGT distributions of Paleogene lignite. The reported lignite samples’ paleolatitudes are located within 57 _S to 48 _N, outside the Arctic region. Is there any lignite record from the Arctic that could be a more direct source to constrain the isoGDGTs distribution? If not, then how can this anomalous abundance of terrestrial isoGDGTs be explained in the Arctic where terrestrial input (especially from peats) is highly suggested while it has not been recorded elsewhere?
REPLY: We are not aware of any study that describes such high abundances of GDGT-3 nor a study that describes GDGT distributions from a northern high latitude Paleogene lignite, such as those described by Suan et al. (2017). In addition, we do not argue that peats are the main contributor to the terrestrial isoGDGT contribution. We merely include this exercise as a crude model for the potential terrestrial contribution to the isoGDGT pool in our ACEX samples, as we will better explain in the next version of the manuscript. Ideally, the analyses we perform here are also conducted using the abundance of isoGDGTs relative to brGDGTs in mineral soils to provide an even more complete picture, but those paired data are not available.

Line 486-487: add the threshold value of GDGT-2/Cren (Weijers et al., 2011), as it is shown as MI’s cutoff in the following.
REPLY: As far as we are aware, a formal threshold or cut off was never defined, but our values are clearly within the safe range of values described by Weijers et al. (2011), which is what we indicated here.

Line 492: I suggest the authors add a short interpretation of why these biomarker results are contrasted to the suitable depositional environment for abundant anaerobic archaea (methanotrophy and methanogen) which they indicated in the beginning of the section.
REPLY: this has been done

Line 508-510: interpreting BIT index with a distal position from the shoreline is problematic. Even in coastal marine or lacustrine settings, the BIT shows a large variation (Hopmans et al., 2004). Is the change of position interpreted from sea-level rise, similar to Sluijs et al. (2006)? Then what caused the sea-level rise (thermal expansion?) while the temperature proxy does not indicate significant warming?
REPLY: We do not only rely on the BIT index but also on palynological evidence that is consistent with a relative drop in terrestrial organic matter contribution. Relative sea level rise is clearly the simplest explanation for the observed changes. Sluijs et al. (2006) described sea level rise during the PETM that was

later shown to be eustatic (Sluijs et al., 2008a). The interval described here regards an episode of relative sea level rise some time before ETM2. We are not aware of literature that has seen similar relative sea level rise elsewhere so we presume this relative sea level rise was of local, perhaps tectonic, origin. We have rephrased as follows:

"At ~371.2 mcd a drop in BIT index and a change in the palynological assemblages corresponds to an interval of greenish sediment, suggestive of pronounced amounts of glauconite. These changes are consistent with local relative sea level rise, causing a somewhat more distal position relative to the shoreline. However, the sediment remains dominantly siliciclastic and organic terrestrial components, particularly pollen and spores, remain abundant still indicating a shallow setting (Sluijs et al., 2008a; Sluijs et al., 2008b)."

Line 591: suggest the citation as "Figure 7b". This applies to other figure citations in the text to be more specific, when available, rather than just citing the whole figure. Another example is - line 606 to change to "Figure 7d"
REPLY: this has been done

Line 633-635: suggest to divide the two methods with (1) and (2), which the dashed line makes it confusing, and remove the linear/non-linear calibration description since these are already explained previously.
REPLY: We have included the 1) and 2) suggestion but we choose to keep the reminder to the reader regarding the linear vs non-linear calibrations.

Line 739: I find "lower temperature mean annual air temperature" very unclear.
REPLY: We have deleted the first 'temperature' to solve this issue.

Figure 1: (1) the word 'using' is used repeatedly – remove or organize with a different word (2) add gplate webpage link for the readers and reference (3) describe or indicate what the brownish lines in the map
REPLY: We have rephrased the caption accordingly

Figure 2: (1) I suggest removing GDGT-4 since it is not discussed in the text nor measured in this study (see supplementary spreadsheet). Moreover, GDGT-4 is generally not included when calculating the relative fraction of isoGDGTs among the whole isoGDGTs pool. (2) add Crenarchaeol regioisomer's structure or note together with the Crenarchaeol (3) suggest changing "chemical structure" to "molecular structure"
REPLY: We have changed the MS accordingly. Specifically, we have removed isoGDGT-4 from the figure as suggested. We noted in the caption of figure 2 that the Crenarchaeol isomer differs from Crenarchaeol in the stereochemistry of a cyclopentane moiety (Sinninghe Damsté et al., 2018), and replaced 'chemical' with 'molecular' as suggested.

Figure 5: (1) describe the "modern peats" into two in the caption. (2) describe what the box and line, error bar, circles indicate (3) add the number of samples for statistical meaning
REPLY: this has been done

Figure 7: (1) I suggest 7d and 7e switch the order, since it is the
REPLY: this has been done

Supplementary material Data table: (1) a lot of blanks in the sample data, as well as an unknown words or sample core names below the data seat (see row 153-157).
REPLY: These open fields in the spread sheet of the raw data have been marked 'below detection' in the revised supplement.

(2) in "iGDGTs in peats" sheet, cite the references
REPLY: this has been done

(3) in "Lignite crenarchaeol", Sluijs et al. reported the GDGTs (iso- and br-) data originally from Naaf et al. (2018) and their newly measured 'Cren. Isomer'. Here, I suggest the authors to report the other iso and br-GDGTs abundances (here which I assume is HPLC/MS integrated peak area) together since they clearly

mentioned in 'Material and Methods' that they re-analyzed the polar fraction of the lignite samples. Although I expect that this will not significantly change the result, still comparing only the newly measured 'Cren. Isomer' with reported GDGT dataset is not acceptable. This is because even measuring the same sample in the same method, the peak area can be different among interlaboratory measurements, the analytical parameter of the analytical instrument etc.
REPLY: We did not re-analyse these samples, but instead revisited the original chromatograms where we determined the peak area for the crenarchaeol isomer (i.e., Naafs et al., 2018). We have amended the text to make this clearer.

In addition, I suggest to add the calculations and results of the 'fraction of isoGDGTs' in all lignite samples. Lastly, minor comment on style of the table (e.g. missing cell borders, missing compound names) to be consistent. Describe 'n.d.' and 'b.d' too.
REPLY: We have added steps in our calculated values for fraction of isoGDGTs in lignites to our data supplement. In addition, to further facilitate reproducibility, we added an example calculation of the data presented in Supplementary Figure 1 and include the meaning of the abbreviations.

Reviewer #2; Dr. Tom Dunkley-Jones

We thank Dr. Dunkley-Jones for his review of our paper. He raises two points. Point 1 regards an as yet unpublished paper by Eley et al., and Point 2 regards the shape of the calibration between SST and TEX_{86}. We discuss these points below.

This is an excellent and thorough reassessment of organic biomarker temperature records for the latest Paleocene and early Eocene, derived from sediments recovered from the central Arctic Ocean. As demonstrated within the manuscript, this time of peak Cenozoic warmth is a key interval of interest to the paleoclimate community. Considerable proxy data and climate model efforts are focusing on this interval to address questions of climate sensitivity and the persistent problem of extreme polar warmth, which is indicated by the proxy data but is still problematic for climate model simulations. The late Paleocene to early Eocene also includes multiple hyperthermal events with millennial-scale onsets, which allow for the study of climate warming and ecosystem responses that approach the rates of modern environmental change. Two of these hyperthermal events are recovered within the ACEX record (PETM and ETM2). The biomarker-based temperature data from the Lomonosov Ridge is a critical latitudinal "end-member" for an assessment of polar warmth during the latest Paleocene and early Eocene. The unusual GDGT assemblages extracted from these samples, and the initial efforts to use these to estimate sea surface temperatures – which by necessity were non-standard – left some concern within the community about their reliability as predictors of absolute temperatures. This study re-evaluates this critical record with new analyses, including of glycerol monoalkyl glycerol tetraethers (GMGTs), and places this new data within the context of the past decade of studies on the calibration and use of GDGT-based thermometry.

Reply: We thank Dr. Dunkley-Jones for his support of our work.

Point 1. This study should be accepted for publication in Climates of the Past, although I do have one recommendation that I would like the authors to consider engaging with. Within this study they do a very thorough job of testing the potential controls and biases on GDGT assemblages using a range of indices and co-occurring markers for terrestrial-derived brGDGTs. The general aim of this is to screen GDGT assemblages, such that they can be separated into those that are formed in broadly analogous conditions to the modern marine system – and hence where the modern temperature dependency of assemblage composition can be well-modelled by the modern core-top calibration - and those samples where the GDGT assemblage is significantly altered, by terrestrial input, methanogenesis or other processes, such that resultant estimates of SSTs may be biased. In their comprehensive treatment of this question of non analogue behaviour and biases, my only recommendation is that the authors also consider the methods proposed by Eley et al. (Climates of the Past Discussions, 2019) for the detection of ancient GDGT assemblages that are significantly non-analogue to the modern calibration dataset. Below I include calculations of their Dnearest metric and OPTiMAL SST estimation for the new GDGT data presented by Sluijs et al. These results confirm some of the key findings of Sluijs et al. – that the pre-PETM GDGT assemblages are anomalous relative to the modern calibration dataset (Dnearest> 1); that there two clear shifts towards GDGT assemblages more "typical" of the modern at _385.0m, and then again at _375.0m. There is also an interval after the PETM, where TEX86 based temperatures remain high (>20_C), whilst OPTiMAL temperatures are considerably lower, with values in the high single figures (_375 to 371 mcd). Sluijs et al. show that pre-ETM2 GDGTs have high BIT indices (_377 to _371 m) and do not consider TEX86 derived temperatures from this interval to be robust because of the potential bias from terrestrial-derived material. The OPTiMAL methodology, however, indicates that these pre-ETM2 GDGT assemblages are relatively closely analogous to GDGT assemblages in the modern core top data (Dnearest <0.5), and that these "near neighbours" are formed in locations with modern MAT SSTs below 10_C.

The Eley et al. (2019) methodology – and the one applied by me below (Figure 1) – includes all modern core top data within the Tierney & Tingley (2015) database, including Arctic data associated with SSTs <3_C. These data were excluded from the standard BAYSPAR calibration ("NoNorth" / "TT13" model of Tierney & Tingley, 2014), because in the Arctic region "TEX86 has a near-zero sensitivity to SST and therefore little predictability" and "incorporation of these data can negatively affect TEX86 predictability in the North Atlantic" (Tierney & Tingley, 2014). Although it would need to be tested – with OPTiMAL being run with and without these modern high-latitude data points and then applied to the ACEX core – it is possible that modern Arctic GDGT assemblages are the "nearest neighbours" of the pre-ETM2 GDGT assemblages, whereas above _371 mcd, assemblages shift to a more normal open marine assemblage, as inferred by Sluijs et al. on the basis of BIT indices. This may, in part, account for the significant warming suggested by OPTiMAL across this transition, and further work would be needed to investigate the inclusion or exclusion of modern Arctic GDGT assemblages in the modern calibration for OPTiMAL, and the ability to extract temperature information from these GDGT assemblages using proxy formulations other than the TEX86 index. Regardless of this, the consideration of the OPTiMAL approach con- firms - through an independent approach that is agnostic about the form or "model choice", of the GDGT – SST relationship - that Arctic SSTs around ETM2 were in the region of _20_C (OPTiMAL) or higher (TEX86H, BAYSPAR).

Reply to point 1. *We are aware of the Eley et al. manuscript and their new indicators are certainly potentially interesting for this paper. As far as we can see on the CP website, however, this paper is under evaluation and, considering the online discussion, may be subject to significant revisions. This compromises the use of this method in its present form.*

We have nevertheless considered the Dnearest and OPTiMAL records kindly provided by the reviewer. Certainly, as the reviewer indicates, some of the results are consistent with our results (e.g. during the latest Paleocene) and could in principle be used as support for our statements. Other aspects are inconsistent with what we find. For example, the interval 377-371 m discussed by the reviewer is particularly interesting. Although the Dnearest metric suggests that TEX_{86} values are robust, the delta Ring Index, a simple metric to evaluate whether GDGT distributions are similar to modern ocean core top data (Zhang et al., 2011), clearly indicates the GDGT assemblage is compromised for reliable TEX86 paleothermometry. The BIT index (>0.4 to 0.8), the palynological assemblage (dominated by terrestrial organic matter) the dinoflagellate cyst assemblage (almost completely freshwater-tolerant) and bulk organic carbon stable carbon isotope ratios are also inconsistent with a dominant marine source of the organic matter (Sluijs et al., 2008b; Sluijs et al., 2009; Sluijs and Dickens, 2012). This would call into question the reliability of the Dnearest metric as an indicator of "normal" marine isoGDGT assemblages, even if they are consistent with some of the modern core top data. Therefore, it seems to us that any discussion on this topic would rather serve as a test to the as yet unpublished new methods proposed by Eley et al. rather than contributing to the main goal of our paper, to reconstruct late Paleocene – early Eocene Arctic paleotemperature.

Collectively, we therefore prefer to not discuss these results at this point.

Point 2. Section 2.1 and especially Lines 145 – 147: suggest that culture and mesocosm experiments and surface sediment data indicate a linear relationship but without a clear citation of these studies. Rather, the citations seem to be of the studies that demonstrate a deviation from linearity. As the authors implicitly acknowledge - with statements like "suggest a linear relation" (line 146) or "assumes a linear relationship" (line 160) - the most appropriate form of the TEX86 – SST relationship is uncertain, with current calibration models making some degree of assumption about the best fit relationship between core top TEX86 data and SSTs. I would suggest a slight rephrase to acknowledge this uncertainty and appropriate citations to back up any arguments made about the form of the relationship. There is extensive discussion of the assumptions that can be made about the form of the TEX86 – SST relationship within the online discussion to Eley et al. (2019) that address this issue, between those who argue for an assumed linear response (Tierney) and those who question this assumption (Eley et al.) – some of the relevant response to Tierney quoted below from Eley et al. (https://www.climpast-discuss.net/cp-2019-60/cp-2019-60-AC1-supplement.pdf):

"We agree that there is a basic underlying trend for more rings within GDGT structures at higher temperatures (Zhang et al. 2015; Qin et al., 2015). What we dispute is that this translates into a simple linear model at the community scale (core top calibration dataset), or is yet reproduced with consistency between strains in laboratory cultures, including the temperature-dependence of GDGT ring numbers within the marine, mesophilic Thaumarchaeota in Marine Group 1 (broadly equivalent to the old Crenarchaeota Group 1) (Eilling et al., 2015; Qin et al., 2015; Wuchter et al., 2007). Wuchter et al. (2004) and Schouten et al. (2007) show a compiled linear calibration of TEX86 against incubation temperature (up to 40_C in the case of Schouten et al., 2007) based on strains that were enriched from surface seawater collected from the North Sea and Indian Ocean respectively. Like Qin et al., (2015) we note the nonlinear nature of the individual experiments in Wuchter et al., 2004 (see Wuchter et al., 2004 Fig. 5). Moreover, the relatively lower Cren' in these studies yield a very different intercept and slope (compared to core-top calibrations e.g. Kim et al. 2010) meaning that the resulting calibrations for TEX86 cannot be applied to core-tops. This was recognised by Kim et al. (2010), who state "but we may speculate that Marine Group I Crenarchaeota species in the enrichment cultures are not completely representative of those occurring in nature…

…As we state above, although we agree that there is a basic underlying trend of increasing ring number with increasing growth temperature, we do not agree that this is well enough known to be quantified into a "basic relationship" that can be "enforced" as a particular model form. Rather, there is uncertainty in the appropriate form of the relationship even within the modern calibration data (see Kim et al. 2010) which becomes substantial beyond the calibration range. The spatial structuring of residuals in global models of modern TEX86 temperature dependence (Tierney & Tingley, 2014) and clear structuring of residuals with temperature in our and other GDGT- temperature calibrations, are likely indications of transitions in the ecology, community make-up or habitat of modern GDGT producers that are not well constrained. We argue that this complexity in the GDGT temperature responses in the modern oceans should be grounds for caution when applying empirical models from the modern to ancient conditions, especially when working with the subset of ancient assemblage data for which there is no modern analogue."

Reply to point 2. *We fully agree with the reviewer here. In fact, some of us have argued for the possibility of a non-linear relation ourselves in a recent paper (Cramwinckel et al., 2018). We will adapt the text in section 2.1 to fully reflect the current status of the discussion (e.g., Hollis et al., 2019).*

References

Cramwinckel, M. J., Huber, M., Kocken, I. J., Agnini, C., Bijl, P. K., Bohaty, S. M., Frieling, J., Goldner, A., Hilgen, F. J., Kip, E. L., Peterse, F., van der Ploeg, R., Röhl, U., Schouten, S., and Sluijs, A.: Synchronous tropical and polar temperature evolution in the Eocene, Nature, 559, 382-386, 10.1038/s41586-018-0272-2, 2018.

Hollis, C. J., Dunkley Jones, T., Anagnostou, E., Bijl, P. K., Cramwinckel, M. J., Cui, Y., Dickens, G. R., Edgar, K. M., Eley, Y., Evans, D., Foster, G. L., Frieling, J., Inglis, G. N., Kennedy, E. M., Kozdon, R., Lauretano, V., Lear, C. H., Littler, K., Lourens, L., Meckler, A. N., Naafs, B. D. A., Pälike, H., Pancost, R. D., Pearson, P. N., Röhl, U., Royer, D. L., Salzmann, U., Schubert, B. A., Seebeck, H., Sluijs, A., Speijer, R. P., Stassen, P., Tierney, J., Tripati, A., Wade, B., Westerhold, T., Witkowski, C., Zachos, J. C., Zhang, Y. G., Huber, M., and Lunt, D. J.: The DeepMIP contribution to PMIP4: methodologies for selection,

compilation and analysis of latest Paleocene and early Eocene climate proxy data, incorporating version 0.1 of the DeepMIP database, Geosci. Model Dev., 12, 3149-3206, 10.5194/gmd-12-3149-2019, 2019.
Naafs, B. D. A., McCormick, D., Inglis, G. N., and Pancost, R. D.: Archaeal and bacterial H-GDGTs are abundant in peat and their relative abundance is positively correlated with temperature, Geochim Cosmochim Ac, 227, 156-170, https://doi.org/10.1016/j.gca.2018.02.025, 2018.
Sinninghe Damsté, J. S., Rijpstra, W. I. C., Hopmans, E. C., den Uijl, M. J., Weijers, J. W. H., and Schouten, S.: The enigmatic structure of the crenarchaeol isomer, Org Geochem, 124, 22-28, https://doi.org/10.1016/j.orggeochem.2018.06.005, 2018.
Sluijs, A., Schouten, S., Pagani, M., Woltering, M., Brinkhuis, H., Sinninghe Damsté, J. S., Dickens, G. R., Huber, M., Reichart, G.-J., Stein, R., Matthiessen, J., Lourens, L. J., Pedentchouk, N., Backman, J., Moran, K., and The Expedition 302 Scientists: Subtropical Arctic Ocean temperatures during the Palaeocene/Eocene thermal maximum, Nature, 441, 610-613, 2006.
Sluijs, A., Brinkhuis, H., Crouch, E. M., John, C. M., Handley, L., Munsterman, D., Bohaty, S., M., Zachos, J. C., Reichart, G.-J., Schouten, S., Pancost, R. D., Sinninghe Damsté, J. S., Welters, N. L. D., Lotter, A. F., and Dickens, G. R.: Eustatic variations during the Paleocene-Eocene greenhouse world, Paleoceanography, 23, PA4216, doi:10.1029/2008PA001615, 2008a.
Sluijs, A., Röhl, U., Schouten, S., Brumsack, H.-J., Sangiorgi, F., Sinninghe Damsté, J. S., and Brinkhuis, H.: Arctic late Paleocene–early Eocene paleoenvironments with special emphasis on the Paleocene-Eocene thermal maximum (Lomonosov Ridge, Integrated Ocean Drilling Program Expedition 302), Paleoceanography, 23, PA1S11, doi:10.1029/2007PA001495, 2008b.
Sluijs, A., Schouten, S., Donders, T. H., Schoon, P. L., Röhl, U., Reichart, G. J., Sangiorgi, F., Kim, J.-H., Sinninghe Damsté, J. S., and Brinkhuis, H.: Warm and Wet Conditions in the Arctic Region during Eocene Thermal Maximum 2, Nature Geoscience, 2, 777-780, 2009.
Sluijs, A., and Dickens, G. R.: Assessing offsets between the $\delta^{13}C$ of sedimentary components and the global exogenic carbon pool across Early Paleogene carbon cycle perturbations, Global Biogeochemical Cycles, 26, GB4005, doi:10.1029/2011GB004224, 2012.
Suan, G., Popescu, S.-M., Yoon, D., Baudin, F., Suc, J.-P., Schnyder, J., Labrousse, L., Fauquette, S., Piepjohn, K., and Sobolev, N. N.: Subtropical climate conditions and mangrove growth in Arctic Siberia during the early Eocene, Geology, 45, 539-542, 10.1130/g38547.1, 2017.
Weijers, J. W. H., Lim, K. L. H., Aquilina, A., Sinninghe Damsté, J. S., and Pancost, R. D.: Biogeochemical controls on glycerol dialkyl glycerol tetraether lipid distributions in sediments characterized by diffusive methane flux, Geochemistry, Geophysics, Geosystems, 12, doi:10.1029/2011GC003724, 2011.

Late Paleocene – early Eocene Arctic Ocean Sea Surface Temperatures: reassessing biomarker paleothermometry at Lomonosov Ridge

Deleted: ;

Appy Sluijs[1], Joost Frieling[1], Gordon N. Inglis[2 *], Klaas G.J. Nierop[1], Francien Peterse[1], Francesca Sangiorgi[1] and Stefan Schouten[1,3]

[1]Department of Earth Sciences, Faculty of Geosciences, Utrecht University. Princetonlaan 8a, 3584 CB Utrecht, The Netherlands

[2]Organic Geochemistry Unit, School of Chemistry, School of Earth Sciences, University of Bristol, Bristol, UK

[3]NIOZ Royal Institute for Sea Research, Department of Microbiology and Biogeochemistry, and Utrecht University, PO Box 59, 1790AB Den Burg, The Netherlands

[*] present address: School of Ocean and Earth Science, National Oceanography Centre Southampton, University of Southampton, UK

Abstract

A series of papers shortly following Integrated Ocean Drilling Program Arctic Coring Expedition (ACEX, 2004) on Lomonosov Ridge indicated remarkably high early Eocene sea surface temperatures (SST; ca. 23 to 27 °C) and land air temperatures (ca. 17 to 25 °C) based on the distribution of isoprenoid and branched glycerol dialkyl glycerol tetraether (isoGDGT and brGDGT) lipids, respectively. Here, we revisit these results using recent analytical developments – which have led to improved temperature calibrations and the discovery of new temperature-sensitive glycerol monoalkyl glycerol tetraethers (GMGTs) – and currently available proxy constraints. The isoGDGT assemblages support temperature as the dominant variable controlling TEX_{86} values for most samples. However, contributions of isoGDGTs from land, which we characterize in detail, complicate TEX_{86} paleothermometry in the late Paleocene and part of the interval between the Paleocene-Eocene Thermal Maximum (PETM; ~56 Ma) and Eocene Thermal Maximum 2 (ETM2; ~54 Ma). Background early Eocene SSTs generally exceeded 20 °C, with peak warmth during the PETM (~26 °C) and ETM2 (~27 °C). We find abundant branched GMGTs, likely dominantly marine in origin, and their distribution responds to environmental change. Further modern work is required to test to what extent temperature and other environmental factors determine their distribution.

Published Arctic vegetation reconstructions indicate coldest month mean continental air temperatures of 6-13 °C, which reinforces the question if TEX_{86}-derived SSTs in the Paleogene Arctic are skewed towards the summer season. The exact meaning of TEX_{86} in the Paleogene Arctic thus remains a fundamental issue, and one that limits our assessment of the performance of fully-coupled climate models under greenhouse conditions.

Deleted: The Integrated Ocean Drilling Program Arctic Coring Expedition on Lomonosov Ridge, Arctic Ocean (IODP Expedition 302 in 2004) delivered the first Arctic Ocean sea surface temperature (SST) and land air temperature (LAT) records spanning the Paleocene-Eocene Thermal Maximum (PETM; ~56 Ma) to Eocene Thermal Maximum 2 (ETM2; ~54 Ma). The distribution of glycerol dialkyl glycerol tetraether (GDGT) lipids

Deleted: indicated elevated SST

Deleted: LATs

Deleted:)

Deleted: However,

Deleted:

Deleted: : i)

Deleted: ii)

Deleted: . Here, we have analyzed GDGT and GMGT distributions in the same sediment samples using new analytical procedures, interpret the results following the

Deleted: and assess the fidelity of new temperature estimates in our study site

Deleted: The influence of several confounding factors on TEX_{86} SST estimates, such as variations in export depth and input from exogenous sources, are typically negligible

Deleted: PETM

Deleted: The isoGDGT distribution further supports temperature as the likely variable controlling TEX_{86} values and w…e conclude that b
e conclude that b

Deleted: e conclude that b

Deleted: ing

Deleted: also report high

Deleted: ces of

Deleted: branched glycerol monoalkyl glycerol tetraethers ... [1]

Deleted:)

Deleted: most

Deleted: show that

Deleted: is sensitive

Deleted: parameters

Deleted: analytical, provenance and environmental

Deleted: if and

Deleted: may be an important factor

Deleted: temperature constraints from branched GDGTs ... [2]

Deleted: proxies

Deleted: ing

Deleted: continental

Deleted: . If

Deleted: truly represent mean annual SSTs, the seasonal ... [3]

Deleted: , seasonal ranges were comparable to those ... [4]

Deleted: exactis uncertaintyfunctioning of

1. Introduction

The Eocene epoch (56 to 34 million years ago; Ma) has long been characterized by warm climates. The earliest signs of a balmy Eocene Arctic region – fossil leaves of numerous plant species – were documented 150 years ago (Heer, 1869). Subsequent findings identified palms, baobab and mangroves, indicating the growth of temperate rainforests and year-round frost-free conditions in the Eocene Arctic region (Schweitzer, 1980; Greenwood and Wing, 1995; Suan et al., 2017; Willard et al., 2019). Fossils of animals, including varanid lizards, tortoises and alligators also indicate warm Arctic climates (Dawson et al., 1976; Estes and Hutchinson, 1980). These earliest findings sparked interest into the climatological mechanisms allowing for such polar warmth about a century ago (Berry, 1922). Ever since, paleobotanists have focused on the Arctic plant fossils and have significantly refined their paleoclimatological interpretation towards estimates of precipitation as well as seasonal and mean annual temperature (e.g. Uhl et al., 2007; Greenwood et al., 2010; Eberle and Greenwood, 2012; Suan et al., 2017; Willard et al., 2019).

Novel insights in Paleogene Arctic paleoclimate research were made in the years following the Arctic Coring Expedition 302 (ACEX, Integrated Ocean Drilling Program (IODP) 2004, Figure 1). This expedition recovered upper Paleocene and lower Eocene siliciclastic sediments, deposited in a shallow marine environment, in Hole 4A (87° 52.00 'N; 136° 10.64 'E; 1,288 m water depth), on the Lomonosov Ridge in the central Arctic Ocean (Backman et al., 2006). The succession was deposited at a paleolatitude of ~78 °N, based on a geological reconstruction (Seton et al., 2012) projected using a paleomagnetic reference frame (Torsvik et al., 2012) (see paleolatitude.org, Van Hinsbergen et al., 2015). The sediments are devoid of biogenic

Deleted: ,

calcium carbonate, but rich in immature organic matter, including terrestrial and marine microfossil assemblages and molecular fossils (e.g. Pagani et al., 2006; Sluijs et al., 2006; Stein et al., 2006).

As the upper Paleocene and lower Eocene sediments of the ACEX core lack biogenic calcium carbonate and alkenones, SST reconstructions are based on the biomarker-based paleothermometer TEX_{86}. This proxy is based on membrane lipids (isoprenoid glycerol dibiphytanyl glycerol tetraethers; isoGDGTs) of Thaumarchaeota, which adapt the fluidity of their membrane according to the surrounding temperature by increasing the number of cyclopentane rings at higher temperatures (De Rosa et al., 1980; Wuchter et al., 2004; Schouten et al., 2013, and references therein). The proxy was introduced in 2002 by Schouten et al. (2002) and was calibrated to mean annual SST using modern marine surface sediments.

Initial papers suggested that Arctic SST increased significantly during two episodes of transient global warming. Maximum values of ~23°C and ~27 °C occurred during the Paleocene-Eocene Thermal Maximum (PETM-56 Ma ago, Sluijs et al., 2006) and Eocene Thermal Maximum 2 (ETM2-54 Ma ago, Sluijs et al., 2009), respectively. Lower SSTs, generally exceeding 20 °C, characterized the remainder of the early Eocene (Sluijs et al., 2008b). Such temperatures were immediately recognized to be remarkably high and could not be explained using fully-coupled climate model simulations (Sluijs et al., 2006). Even the current-generation of IPCC-class models are unable to match early Eocene Arctic mean annual SSTs, although reconstructions of tropical and mid-latitude SSTs and deep ocean temperatures are consistent with some newer simulations (Frieling et al., 2017; Cramwinckel et al., 2018; Evans et al., 2018; Zhu et al., 2019).

Deleted: }} that provided a wealth of information regarding Paleocene and Eocene Arctic climates, environments, and ecosystems (Brinkhuis et al., 2006; Pagani et al., 2006; Sluijs et al., 2006; Stein et al., 2006; Schouten et al., 2007b; Stein, 2007; Sangiorgi et al., 2008; Sluijs et al., 2008b; Waddell and Moore, 2008; Weller and Stein, 2008; Sluijs et al., 2009; Speelman et al., 2009; Speelman et al., 2010; Barke et al., 2011; Barke et al., 2012; Krishnan et al., 2014; Willard et al., 2019)…

Deleted: cyclisations

Since the publication of the ACEX SST records, constraints on the applicability of the TEX_{86} proxy have tremendously improved (see review by Schouten et al., 2013, and subsequent work by Taylor, 2013 #1645; Elling et al., 2014; Qin et al., 2014; Elling et al., 2015; Kim et al., 2015; Qin et al., 2015; Hurley et al., 2016; Zhang et al., 2016). This work has delivered new constraints on the ecology of Thaumarchaeota, the dominant depth at which they reside in the ocean and from which depth their isoGDGTs are exported towards the sea floor. It also identified potential confounding factors such as variation in dominant isoGDGT export depth (e.g., Taylor et al., 2013; Kim et al., 2015), the input of non-Thaumarchaeotal-derived isoGDGTs (e.g., Weijers et al., 2011; Zhang et al., 2011), growth phase (Elling et al., 2014), and environmental ammonium and oxygen concentrations (Qin et al., 2015; Hurley et al., 2016). Moreover, several indicators to detect such anomalies have been developed. Improvements in the chromatography method used for GDGT analysis now allow for better separation of previously co-eluting compounds leading to enhanced analytical precision and sensitivity (Hopmans et al., 2016). Finally, recent work has described new GDGTs from oceans and sediments, notably branched glycerol monoalkyl glycerol tetraethers (brGMGTs, or 'H-shaped' brGDGTs) (e.g., Schouten et al., 2008; Liu et al., 2012), characterized by a covalent carbon-carbon bond that links the two alkyl chains. Their presence and distribution in peats and lake sediments has been linked to land air temperatures (LAT) (e.g., Naafs et al., 2018a; Baxter et al., 2019). However, these compounds have not yet been reported from ancient marine sediments.

Considering these developments and the paleoclimatological importance of the ACEX dataset, we re-analyzed the original lipid extracts for the PETM, ETM2 and the interval spanning these events (Sluijs et al., 2006; Sluijs et al., 2009), according to the latest chromatography protocols. We also compile published and generate new GDGT data

Deleted: Moreover, i

Deleted: and

Deleted: n addition, i

Deleted: improved

Deleted: Also

Deleted: brGMGTs

Deleted: , previously or

Deleted: br

Deleted: , that may be useful for reconstructing land

Deleted: investigated in

from modern and Paleogene terrestrial deposits and use these to better assess the potential confounding influence of isoGDGTs from terrestrial sources, which was already recognized as a potential problem in the early work (Sluijs et al., 2006).

2. GDGT-based SST indices, calibration and confounding factors

2.1 TEX_{86} and its calibration to SST

TEX_{86} is based on the relative abundance of 4 different GDGTs (Figure 2), following (Schouten et al., 2002):

$$TEX_{86} = \frac{([GDGT-2]+[GDGT-3]+[Crenarchaeol\ isomer])}{([GDGT-1]+[GDGT-2]+[GDGT-3]+[Crenarchaeol\ isomer])} \quad \text{Eq. (1)}$$

where a higher relative abundance of cyclopentane moieties implies higher SSTs.

A number of models are used to calibrate TEX_{86} to SST (Schouten et al., 2002; Schouten et al., 2003; Schouten et al., 2007; Kim et al., 2008; Liu et al., 2009; Kim et al., 2010; Tierney and Tingley, 2014; O'Brien et al., 2017), all based on a modern ocean surface sediment database. The currently available culture and mesocosm experiments and surface sediment data suggest that the relation between SST and TEX_{86} is close to linear for a large portion of the modern ocean (Kim et al., 2010; Ho et al., 2014; Tierney and Tingley, 2014; O'Brien et al., 2017). In polar regions, the TEX_{86} response to temperature diminishes (e.g., Kim et al., 2010; Tierney and Tingley, 2014). The response of TEX_{86} to SST at the high temperature end remains subject of discussion (e.g. Cramwinckel et al., 2018; Hollis et al., 2019). Several authors prefer a linear relation (e.g., Tierney and Tingley, 2014; O'Brien et al., 2017). However, physiological considerations and multiple temperature-dependent GDGT indices might imply a non-linear relation also at the high temperature end, as can be observed at the high end of the modern ocean dataset and beyond the reach of the modern ocean in paleoclimate

Deleted: indeed

Deleted: a linear relation, except for

Deleted: where

Deleted: deviates

data (Cramwinckel et al., 2018). At higher temperatures, membrane adaptation may increasingly be established using isoGDGTs not included in the TEX_{86} ratio leading to a diminished TEX_{86} response at very high temperatures (Cramwinckel et al., 2018). A non-linear response has thus been proposed in other calibrations (Liu et al., 2009; Kim et al., 2010). The most recent non-linear calibration, TEX_{86}^{H} (Kim et al., 2010), represents an exponential relation between SST and TEX_{86} (Hollis et al., 2019). Unfortunately, TEX_{86}^{H} is mathematically problematic and has systematic residuals in the modern ocean (Tierney and Tingley, 2014).

Tierney and Tingley (2014) introduced a spatially-varying Bayesian method to convert TEX_{86} to SST and assumes a linear relationship (BAYSPAR). BAYSPAR extracts TEX_{86} values from the modern core-top dataset that are similar to the measured TEX_{86} value from the geological sample based on a tolerance defined by the user, and subsequently calculates regressions based on these core-top data. The uncertainty in SST reflects spatial differences in the correlation coefficient and intercept and the error variance of the regression model.

Currently, it is generally encouraged to present results both using a linear and a non-linear function (Hollis et al., 2019). The assumption of a linear or non-linear relation between SST and TEX_{86} leads to very different SST reconstructions for geological samples yielding TEX_{86} values >0.70 (Kim et al., 2010; Tierney and Tingley, 2014; Frieling et al., 2017; O'Brien et al., 2017; Cramwinckel et al., 2018; Hollis et al., 2019). However, TEX_{86} values of the early Eocene ACEX samples (0.5 – 0.7, Sluijs et al., 2006; Sluijs et al., 2008b; Sluijs et al., 2009) are below this value and well above most values observed in the polar regions (Kim et al., 2010; Tierney and Tingley, 2014; O'Brien et al., 2017), indicating that all calibrations will yield similar absolute SST values.

Deleted: Specifically, a

Deleted: ,

Deleted: which

Deleted: between the two

Deleted: In deep-time settings,

Deleted: searches

Deleted: the modern core-top dataset for

Deleted: within a user-specified tolerance and draws regression parameters from these

Deleted: modern analogue locations

Deleted: is approach yields uncertainty bounds that reflect

Deleted: slope

Deleted: terms

Deleted: , based on the modern ocean

Deleted: accepted

Deleted: beyond the modern data set

Deleted:)

Deleted: well within the modern ocean calibration dataset

2.2 Caveats and confounding factors

Several confounding factors and caveats have been identified that could potentially bias TEX_{86} data relative to mean annual SST. These notably relate to additions of isoGDGTs that were not produced in the upper water column by Thaumarchaeota, seasonal biases, and choices that are made in the calibration between SST and TEX_{86}. Below we summarize methods that have been developed to assess if isoGDGT distributions might have been biased by confounding factors.

2.2.1 isoGDGTs of terrestrial origin

Previous work (Sluijs et al., 2006; Sluijs et al., 2008b; Sluijs et al., 2009) recognized that high contributions of terrestrially-derived isoGDGTs could compromise the TEX_{86} signal for portions of the upper Paleocene to lower Eocene interval of the ACEX core. This contribution can be tracked using the Branched and Isoprenoid Tetraether (BIT) index, a ratio of mostly soil-derived branched GDGTs (brGDGTs; Figure 2) and Crenarchaeol, which is dominantly marine-derived (Hopmans et al., 2004; Schouten et al., 2013):

$$BIT\ index = \frac{([brGDGT-Ia]+[brGDGT-IIa]+[brGDGT-IIIa])}{([brGDGT-Ia]+[brGDGT-IIa]+[brGDGT-IIIa])+[Crenarchaeol])} \quad \text{Eq. (2)}$$

Most studies define a BIT value (typically 0.3 or 0.4) above which TEX_{86}-derived SST are unreliable (e.g., Weijers et al., 2006). However, the threshold of 0.4 is conservative in some settings and the impact of terrigenous GDGTs on reconstructed SST will depend on the nature and temperature of the source catchment (Inglis et al., 2015). In addition, a cut-off value based on BIT values is difficult given the relatively large differences in BIT between labs, which originate from methodological differences (Schouten et al., 2009). A strong linear relationship between BIT and TEX_{86} values is

Deleted: At the time of the first ACEX papers, it was already known that high contributions of terrestrially-derived isoGDGTs could compromise the TEX_{86} signal (Weijers et al., 2006). …

Deleted: indeed

Deleted: that high terrestrial contributions of isoGDGTs could be problematic

Deleted: based on high BIT index values

Deleted:

often taken as indication of a bias in TEX_{86} through land-derived isoGDGTs to the marine TEX_{86} signature (e.g., Douglas et al., 2014). An earlier study used a somewhat subjective threshold of 0.3 for an interval spanning ETM2 in the ACEX core (Sluijs et al., 2009).

2.2.2 isoGDGTs of deep water origin

Thaumarchaeota, the source of most isoGDGTs in marine waters (Zeng et al., 2019; Besseling et al., 2020), are ammonium oxidizers (Könneke et al., 2005; Wuchter et al., 2006a), making them independent of light. Although they occur throughout the water column, maximum abundances occur at depths <200 m, generally around NO_2 maxima (e.g., Karner et al., 2001; Pitcher et al., 2011a). In most oceans, sedimentary GDGTs dominantly derive from the upper few hundred meters, based on analyses of suspended particular organic matter and sediment traps (Wuchter et al., 2005; Wuchter et al., 2006b; Yamamoto et al., 2012; Richey and Tierney, 2016). A deeper contribution has also been inferred based on ^{14}C analysis (Shah et al., 2008), implying possible contributions of isoGDGTs from thermocline. Moreover, contributions of isoGDGTs produced in the deep sea have regionally been identified (e.g., Kim et al., 2015). Taylor et al. (2013) also found that deep dwelling (>1000 meter) archaea might contribute to the sedimentary isoGDGT assemblage. They indicate that such deep contributions can be tracked using the GDGT-2/GDGT-3 ratio; high values of >5 indicate contributions of archaea living deeper in the water column. Given that upper Paleocene and lower Eocene ACEX sediments were deposited in a shallow shelf environment (Sluijs et al., 2008b), a significant contribution of deep ocean archaeal lipids is not expected.

Deleted: are

Deleted: the

Deleted: ,

Deleted: although some contributions from deeper have sometimes…

Deleted: . This implies

Deleted: produced

Deleted: in

Deleted: waters

Deleted: er

Formatted: Dutch

2.2.3 isoGDGTs of methanotrophic and methanogenic archaea

Contributions of isoGDGTs to the sedimentary pool might also derive from anaerobic methanotrophs and/or methanogens. Several indices have been developed to track such contributions, both based on relatively high contributions of particular isoGDGTs of these groups of archaea. The Methane Index (MI) was developed to detect the relative contribution of anaerobic methanotrophic Euryarchaeota assumed to be represented by GDGT-0 but also GDGT-1, 2 and 3 (Zhang et al., 2011) and is therefore defined as

$$MI = \frac{[GDGT-1]+[GDGT-2]+[GDGT-3]}{([GDGT-1]+[GDGT-2]+[GDGT-3]+[Crenarchaeol]+[Crenarchaeol\ isomer])} \quad \text{Eq. (3)}$$

MI values greater than 0.5 indicate significant contribution of anaerobic methanotrophy. Such values may yield unreliable TEX_{86} values. Another tracer for contributions of anaerobic methanotrophic archaea is the analogous GDGT-2/Crenarchaeol ratio (Weijers et al., 2011).

Methanogenic archaea can synthesize GDGT-0, as well as smaller quantities of GDGT-1, GDGT-2 and GDGT-3. The ratio GDGT-0/Crenarchaeol is indicative of contributions of methanogenic archaea to the isoGDGT pool (Blaga et al., 2009) where values > 2 indicate substantial contribution of methanogenic archaea. Up to now, high index values have often been observed near methane seeps or anoxic basins (e.g., Jaeschke et al., 2012) but rarely in open marine waters in the modern and paleodomains (Inglis et al., 2015; Zhang et al., 2016). Given the reducing conditions in the sediment and water column at the study site across the late Paleocene and early Eocene (Sluijs et al., 2006; Stein et al., 2006; Sluijs et al., 2008b; März et al., 2010), an influence of methane cycling might be expected.

Formatted: Font: Not Italic

Deleted: .

Deleted: ices

2.2.4 isoGDGTs of the 'Red Sea Type'

Sedimentary isoGDGT distributions from the Red Sea are anomalous to other marine settings and are characterised by the low abundance of GDGT-0 and the high abundance of the Crenarchaeol isomer. Presumably, this is due to an endemic Thaumarchaeotal assemblage. The Red Sea isoGDGT distribution yields a different relationship between SST and TEX_{86} (Trommer et al., 2009; Kim et al., 2015). Inglis et al. (2015) attempted to quantify a 'Red Sea-type' GDGT distribution in geological samples using the following index:

Deleted: that of

Deleted: regio-

Deleted: , p

Deleted: , and this

$$\%GDGTrs = \frac{[Crenarchaeol\ isomer]}{([GDGT-0] + [Crenarchaeol\ isomer])} \times 100 \qquad \text{Eq. (4)}$$

However, as noted by Inglis et al. (2015) this ratio is also strongly SST-dependent such that the Red Sea type GDGT assemblage cannot be discerned from GDGT distributions that occur at high temperatures in normal open marine settings.

2.2.5 Seasonal bias

TEX_{86} is calibrated to mean annual SST. However, particularly in mid and high latitude areas where production and export production is highly seasonal, the sedimentary GDGT distribution might not represent annual mean conditions (Wuchter et al., 2006b; Pitcher et al., 2011b; Mollenhauer et al., 2015; Richey and Tierney, 2016; Park et al., 2019). This issue should partly be reflected in the calibration uncertainty of the modern ocean database (several °C, depending on the calibration and method; see section 2.7). Sluijs et al. (2006; 2008b; 2009) originally argued that the TEX_{86} results from the ACEX core could be biased towards summer temperature because the export of organic matter from the surface ocean towards the sediment likely peaked during the season of highest production, i.e., the summer. However, we also note that the TEX_{86}-temperature relationship is not improved when using seasonal mean ocean temperatures (Kim et al., 2010; Tierney and Tingley, 2014) and modern observations indicate homogenization of the seasonal cycle at depth (Wuchter et al., 2006b; Yamamoto et al., 2012; Richey and Tierney, 2016), implying that seasonality has relatively limited effect on modern sedimentary TEX_{86} values.

2.2.6 Additional isoGDGT-based temperature indicators

The underlying mechanism of TEX_{86} is that isoGDGTs produced at higher SSTs contain more rings than those produced at low SSTs. Although the combination of compounds included in TEX_{86} seems to yield the strongest relation with temperature in the modern ocean (Kim et al., 2010), it implies that isoGDGT ratios other than TEX_{86} also provide insights into SST. One alternative temperature sensitive isoGDGT index is the Ring Index (RI), which represents the weighed number of cyclopentane rings of isoGDGTs 0-3, Crenarchaeol and the Crenarchaeol isomer (Zhang et al., 2016), defined as:

$$RI = 0x[\%GDGT-0] + 1\,x[\%GDGT-1] + 2\,x[\%GDGT-2] + 3\,x[\%GDGT-3] + 4\,x\,[\%Crenarchaeol + \%Crenarchaeol\ isomer] \qquad \text{Eq. (5)}$$

Note that the abundance of GDGT-0 is important for determining the percentage of the other GDGTs of the total isoGDGT pool.

The close relation between TEX_{86} and RI can also be used to detect aberrant distributions, including those produced by methanogenic, methanotrophic and terrestrial sources, as these sources typically contribute disproportionate amounts of specific lipids. A RI_{TEX}, calculated from TEX using the polynomial fit of Zhang et al. (2016), is subtracted from the RI to arrive at the ΔRI. Cut-off values for sample deviation from the modern ocean calibration dataset are defined as 95% confidence limits of the RI-TEX relation, or above |0.3| ΔRI units.

2.3 H-shaped branched GDGTs; brGMGTs

BrGMGTs (Figure 2) were first identified by Liu et al. (2012) in marine sediments, who identified a single acyclic tetramethylated brGMGT (*m/z* 1020). This compound was later detected within the marine water column and appeared to be abundant within the oxygen minimum zone (Xie et al., 2014). Naafs et al. (2018a) identified a larger suite of brGMGTs (including *m/z* 1048 and 1034), in a quasi-global compilation of modern peat samples. They argued that these compounds were preferentially produced at depth, within the anoxic catotelm. Analogous to the continental paleothermometer based on bacterial brGDGTs produced in surface soils, termed MBT'$_{5me}$ (Weijers et al., 2007b; De Jonge et al., 2014), they showed that the degree of methylation of brGMGTs in peats relates to mean annual air temperature. They calculated the degree of methylation of brGDGTs without cyclopentane moieties, designed for comparison to the methylation of brGMGTs, defined by H-MBT$_{acyclic}$:

Deleted: ,or H-shaped brGDGTs (hereafter referred to as branched glycerol monoalkyl glycerol tetraethers

$$MBTacyclic = \frac{brGDGT-Ia}{(brGDGT-Ia+brGDGT-IIa+GDGT-IIa'+brGDGT-IIIa+brGDGT-IIIa')} \quad \text{Eq. (6)}$$

$$H-MBTacyclic = \frac{brGMGT-H1020}{(brGMGT-H1020+brGMGT-H1034+brGMGT-1048)} \quad \text{Eq. (7)}$$

Based on the strong relation between MBT$_{acyclic}$ and H-MBT$_{acyclic}$ in their peat samples, Naafs et al. (2018a) suggested that the brGMGTs have the same origin as the brGDGTs, presumably Acidobacteria (Sinninghe Damsté et al., 2011; Sinninghe Damsté et al., 2018a). In addition, they showed that the abundance of brGMGTs (relative to the total amount of brGMGTs and brGDGTs) positively correlates with mean annual air temperature, suggesting that the covalent bond in the brGMGTs is used to maintain membrane stability at higher temperature (Naafs et al., 2018a).

Baxter et al. (2019) identified a total of seven different brGMGTs from a suite of African lake sediments (Figure 2), and found their relative distribution to correlate to mean annual air temperature. Accordingly, they proposed a proxy for mean annual air temperature termed brGMGT-I (see Figure 2 for the molecular structures referred to here):

Deleted: ,

Deleted: in the mass chromatograms with *m/z* 1020, 1034 and 1048 …

$$brGMGT - I = \frac{[H1020c]+[H1034a]+[H1034c]}{[H1020b]+[H1020c]+[H1034a]+[H1034c]+[H1048]} \quad \text{Eq. (8)}$$

3. Material and Methods

We used the polar fractions previously analyzed by Sluijs et al. (2006; 2009) from the PETM through ETM2 interval at IODP Expedition 302 Hole 4A. These fractions originate from a total lipid extract produced using a Dionex Accelerated Solvent Extractor and fraction separations by Al_2O_3 column chromatography using hexane:dichloromethane (DCM) (9:1, *v/v*) and DCM:methanol (1:1; *v/v*) to yield the apolar and polar fractions, respectively. Polar fractions were re-dissolved in hexane:isopropanol (99:1, *v/v*)) and passed through a 0.45-µm polytetrafluoroethylene filter. This fraction was then analyzed by high-performance liquid chromatography (HPLC) and atmospheric pressure chemical ionization–mass spectrometry using an Agilent 1260 Infinity series HPLC system coupled to an Agilent 6130 single-quadrupole mass spectrometer at Utrecht University following Hopmans et al. (2016) to measure the abundance of GDGTs. Based on long-term observation of the in-house standard, the analytical precision for TEX_{86} calculates to ±0.3 °C in the SST domain.

Deleted: is

To gain further insights into the potential impact of terrestrial isoGDGT input on TEX_{86} values, we compiled isoGDGT and brGDGTs distributions from modern peats (n = 473, Naafs et al., 2017) and early Paleogene lignites (n = 58, Naafs et al., 2018b). Note, the fractional abundance of Crenarchaeol isomer was not reported in the early Paleogene dataset of Naafs et al. (2018b). We therefore revisited the original chromatograms from Naafs et al. (2018b) and integrated the crenarchaeol isomer (*m/z* 1292).

4. Results

The new GDGT distributions (Supplementary Table) are consistent with the TEX_{86} and BIT index data generated over a decade ago using the older analytical HPLC setup (Hopmans et al., 2000; Hopmans et al., 2016) (Figure 3). TEX_{86} exhibits some scatter but the slope of the regression is 0.98 for the entire dataset, which is indistinguishable from the 1:1 line. The scatter is minor compared to the uncertainties inherent to calibrations that transfer these values to SST. Less scatter is apparent in the BIT record but the original BIT index values were slightly higher than recorded here (~0.5), indicated by a shallower slope of the regression (0.92). This result is consistent with previous analyses with the new analytical setup (Hopmans et al., 2016). This does not impact previous qualitative interpretations of this record (Sluijs et al., 2006; Sluijs et al., 2008b; Sluijs et al., 2009). In the discussion section, we assess indicators of potential confounding factors (section 2.2), including the influx of terrestrially-derived isoGDGTs to the sediments (Figures 4, 5 and S1) and several indices related to methane and depth of production (Figures 6).

Although we did not detect significant amounts of isoprenoid GMGTs, high abundances of various brGMGTs are present in the ACEX samples, in total between 10 and 45% of the total brGDGT assemblage (Figure 7). We consistently identify at least five brGMGTs across the three different mass-to-charge ratios (*m/z* 1020, 1034 and 1048). Based on their (relative) retention times and overall distribution we were able to

Deleted: We therefore re-analyzed the polar fractions of their early Paleogene lignite extracts via HPLC-MS using a ThermoFisher Scientific Accela Quantum Access at the University of Bristol following Hopmans et al. (2016). Based on long-term observation of the in-house standard, the analytical precision for TEX_{86} is ±0.3 °C for both labs.

Deleted: at the higher end

Deleted: ,

Deleted: , are present in the ACEX samples

Deleted: Specifically, w

Deleted: can

Deleted: 5 peaks across the mass chromatograms of *m/z* apply the nomenclature of Baxter et al. (2019) to five of these and assign individual peaks to previously identified compounds (Figure S2). The abundance of brGMGTs relative to brGDGTs increase during the PETM. The proposed temperature indicators based on brGMGTs show mixed results, with some showing a clear response to the PETM (Figure 7e) while others do not (Figure 7d).

5. Discussion

5.1 IsoGDGT provenance

5.1.1 Contributions of soil-derived isoGDGTs

As noted by Sluijs et al. (2006), late Paleocene samples yield anomalously high abundances of GDGT-3, likely derived from a terrestrial source. We therefore consider the late Paleocene temperature estimates unreliable. To assess the temperature change during the PETM, Sluijs et al. (2006) developed a TEX_{86} calibration without this moiety, termed TEX'_{86}. However, TEX'_{86} has not been widely used outside the Paleogene Arctic because the anomalous abundances of GDGT-3 have not been recorded elsewhere. High contributions of GDGT-3 from terrestrial input would also be associated with an increase in the abundance of other isoGDGTs. Indeed, recent TEX_{86}-based global SST compilations and comparison to climate simulations for the PETM excluded the Paleocene ACEX data because the TEX_{86}' calibration complicates the comparison to other regions where it has not been applied (Frieling et al., 2017; Hollis et al., 2019).

Input of soil organic matter is consistent with Willard et al. (2019) who established that the brGDGT assemblage is dominantly soil-derived as opposed to being produced in the coastal marine environment. This observation is based upon the weighted average number of rings in the tetramethylated brGDGTs (#rings$_{tetra}$) which generally does not

Deleted: 5
Deleted: A
Deleted: s
Deleted: Furthermore, t
Deleted: d
Deleted: e
Deleted: they therefore explored
Deleted: In addition, h
Deleted: We therefore consider the late Paleocene temperature estimates unreliable.
Deleted: record
Deleted: and has not been applied elsewhere
Deleted:
Deleted: {Sinninghe Damsté, 2016 #1997}

exceed 0.4 to 0.7 in the global soil calibration dataset (Sinninghe Damsté, 2016). In the ACEX record, #rings$_{tetra}$ is $\leq$ 0.21 (Willard et al., 2019), consistent with a dominant soil source. This indicates that 1) brGDGT abundances, 2) brGDGT distributions and 3) the BIT index are reliable indicators of the relative supply of terrestrially-derived isoGDGTs into the marine basin. The Paleocene section of the dataset also stands out regarding its relation between BIT index and TEX$_{86}$ (Figure 4), which confirms its anomalous nature.

During the PETM, TEX$_{86}$ values are higher (due to warming) and BIT values lower. This was attributed to sea level rise during the hyperthermals resulting in a more distal position relative to the terrestrial GDGT source (Sluijs et al., 2006; Sluijs et al., 2008a). The interval between 371.0 and 369.0 mcd (i.e. above the PETM and below ETM2) stands out. This interval was previously recognized by Sluijs et al. (2009) to reflect an open marine environment, with a dominance of marine palynomorphs and algal biomarkers. They also found that high BIT values correspond to low TEX$_{86}$ values within that interval and therefore implemented a subjective threshold value of 0.3, above which TEX$_{86}$-derived SSTs were considered unreliable. Although the relation between BIT and TEX$_{86}$ exhibits considerable much scatter, the new analyses supports the notion that higher influx of terrestrial isoGDGTs lowers TEX$_{86}$ values. The linear regression (Figure 4; excluding the one outlier with high TEX$_{86}$ and BIT values in the top right of the plot because it has highly anomalous distributions (ΔRI = 0.61)), yields an R^2 of 0.26 so explains a portion of the variation (Figure 4). The nature of this influence is determined by the relative abundance of terrestrial isoGDGTs and their TEX$_{86}$ value. The TEX$_{86}$ value at the terrestrial endmember of BIT = 1, assuming various types of regressions, centers around 0.5. The remainder of the data does not show a clear relation between BIT and TEX$_{86}$ although some of the lowest TEX$_{86}$

Deleted: always below
Deleted: ,
Deleted: which
Deleted: From t
Deleted: 8
Deleted: , just
Deleted: the most
Deleted: in the studied section
Deleted: dominant
Deleted: they
Deleted: cut-off BIT
Deleted: yields
Deleted: , explaining 26% of the variation in a linear regression…
Deleted: relations

values correspond to high BIT values, suggesting that the terrestrial endmember contributed isoGDGT assemblages with relatively low TEX_{86} values in other intervals as well.

The relatively low degree of cyclization in the early Eocene contrasts starkly with high degree of cyclisation during the late Paleocene (Figure 6). This implies that the distribution of terrestrial isoGDGTs varies strongly between the latest Paleocene and early Eocene within our studied section.

Deleted: Interestingly, t
Deleted: The
Deleted: of soil-derived isoGDGTs
Deleted: the anomalous contributions of GDGT-3 in the
Deleted: supplied
Deleted: differed
Deleted: early
Deleted: within our

The impact of soil-derived isoGDGTs also emerges from the Ring Index approach of Zhang et al. (2016, see section 2.6 and Figure 6). The difference between the Ring Index and TEX_{86} at the onset of the PETM is mainly controlled by Crenarchaeol, which is comparatively low in abundance in the Paleocene but highly abundant in the PETM. This increase is likely associated with sea level rise during the PETM because Crenarchaeol is predominantly produced in the marine realm. It is also consistent with a drop in BIT index values and the relative abundance of terrestrial palynomorphs (Sluijs et al., 2008a). The approach of Zhang et al. (2016) also confirms that many isoGDGT distributions exhibit an anomalous relation between TEX_{86} and the Ring Index relative to the modern core top dataset, with ΔRI values >0.3 (Figure 6). Importantly, all samples with ΔRI values >0.3 have BIT values above 0.35, indicating that contributions of soil-derived iso-GDGTs dominate non-temperature effects in the distributions. We therefore discard TEX_{86}-derived SSTs for samples with BIT values >0.35.

We also develop a crude model to further constrain the potential contribution of terrestrially-derived isoGDGTs. First, we determine the abundance of isoGDGTs relative to brGDGTs in modern peat samples (Naafs et al., 2017) and early Paleogene lignites (fossil peat) (Naafs et al., 2018b, the isoGDGT data are published here).

Deleted: attempt to
Deleted: by
Deleted: ing

Although there is no reason to assume that peat was a major component of the hinterland (Willard et al., 2019) , the aforementioned datasets can provide an estimate of the potential contribution from terrestrial isoGDGTs to our study site. The raw signal intensity of brGDGTs in the ACEX samples are used to estimate the potential contribution of terrestrially-derived isoGDGTs to the samples. To this end, we use the fractional abundance of the various isoGDGTs in the modern peat and Paleogene lignite datasets (Figure 5). Then, we estimate the abundance of these terrestrially-derived isoGDGTs in our ACEX samples by scaling this fraction to the measured abundances of brGDGTs and isoGDGTs in our ACEX samples, following

$$Terrestrial\ fraction\ of\ isoGDGT\ x =$$

$$\left(Fraction\ of\ isoGDGT x\ in\ terrestrial\ test\ dataset * \frac{sum(brGDGTs))}{abundance\ of\ isoGDGT\ x}\right) \quad \text{Eq. (9)}$$

where x represents the specific analyzed GDGT (see Supplementary Data File for an example of these calculations).

This leads to estimates of the potential relative contributions of the individual isoGDGTs derived from land in the ACEX samples based on the entire modern peat dataset (Naafs et al., 2017), modern peats from regions with MAT exceeding 15°C (Naafs et al., 2017) and Paleogene lignites (Naafs et al., 2018b, this paper, Figures 5 and S1). This approach implies that Crenarchaeol and the Crenarchaeol-isomer are almost exclusively from the marine realm. However, GDGT-1, GDGT-2 and GDGT-3 in our study site may be derived from the terrestrial realm (Figure 5), especially in specific stratigraphic intervals (Figure S1). In the most extreme cases, the modeled contributions of terrestrial isoGDGTs is higher than the measured isoGDGT abundances (i.e., terrestrial fraction ≥ 1). This is principally seen in iGDGT-2 and GDGT-3, especially when we employ the Paleogene lignite database. This particular assumption clearly overestimates the abundance of terrestrially sourced isoGDGTs in

Deleted: aforementionedcan nofcontribution from s to our study site
Deleted: absolute concentrations
Deleted: then
Deleted: available global terrestrial sediment calibration datasets, specifically
Deleted: s
Deleted: n
Deleted: n
Deleted: *n*
Deleted: *n*
Deleted: shows
Deleted: remain
Deleted: even with high brGDGT concentrations
Deleted: we show that
Deleted: all have potentially large terrestrial contributions in the ACEX samples
Deleted: more concentrated
Deleted: ,
Deleted: based on the measured brGDGTs and modern peat dataset is …
Deleted: actually
Deleted: higher than
Deleted: and predominantly
Deleted: calculate the isoGDGT contribution using
Deleted: thus
Deleted: leads to
Deleted: of
Deleted: amount

our setting. However, the temporal trends obtained using modern peats, subtropical modern peats and Paleogene lignites are essentially identical and give some indication which isoGDGTs are most likely to be impacted by terrestrial input and across which intervals. Interestingly, this approach also suggests that particularly GDGT-3 is shown to be strongly affected (Figure 5), which qualitatively matches the distributions in the ACEX samples. This is principally because GDGT-3 is the least abundant marine isoGDGT included in our analyses, whereas it is often as abundant as GDGT-1 and 2 in terrestrial settings (Fig. 5).

5.1.2 Contributions of methanotrophic or methanogenic archaea?

The depositional environment at the study site included ample (export) production, sediment organic matter content, and low oxygen conditions at the sediment-water interface (Sluijs et al., 2006; Stein et al., 2006; Stein, 2007; Sluijs et al., 2008b; Sluijs et al., 2009; März et al., 2010). This may have been suitable for abundant methanogenic and methanotrophic archaea, potentially contributing to the sedimentary isoGDGT assemblage. However, our GDGT-2/Crenarchaeol values (<0.23; Figure 6) are far below values that suggest significant isoGDGT contributions of methanotrophic Euryarchaeota as described by Weijers et al. (2011). MI values (maximum observed 0.31) are also generally below proposed cut off values (0.3-0.5, Zhang et al., 2011) that suggest such contributions. Finally, GDGT-0/Crenarchaeol ratios (<1.4) remain below the cut-off value of 2 throughout the section (Figure 6), also making a significant isoGDGT contribution from methanogens highly unlikely (Blaga et al., 2009). Collectively, relative contributions of isoGDGTs from methanogenic and methanotrophic archaea seem low despite the low-oxygen environment, suggesting a relatively high flux of pelagic isoGDGTs.

Deleted: between the

Deleted: warm

Deleted: affected and

Deleted: ¶

Deleted: to

Deleted: be

Deleted: in ACEX samples if the terrestrial contribution of isoGDGTs is analogous in distribution to that of warm modern peats and/or Paleogene lignites

Deleted: , with

Deleted: ,

Formatted: Font: Not Italic

Deleted: Also

5.1.3 Contributions of deep-dwelling archaea?

Taylor et al. (2013) showed that GDGT-2/GDGT-3 ratios correspond to depth of production, with high values (>5) in deep waters (>1000 m). We record low values (1-4) between ~390 and ~371.2 mcd (Figure 6), which supports a dominant production in the surface ocean based on the modern calibration data set (Taylor et al., 2013). However, the overlying interval (~371 to ~368.3 mcd) has much higher (average 7.4) and variable GDGT-2/GDGT-3 values with peak values of 10-14. Such values suggest significant contributions of isoGDGTs produced at water depths of several kilometers according to the analyses by Taylor et al. (2013).

However, all paleoenvironmental information generated based on the sediments as well as tectonic reconstructions of Lomonosov Ridge – a strip of continental crust that disconnected from the Siberian margin in the Paleocene - has indicated a neritic setting of the drill site at least up to the middle Eocene (e.g., O'Regan et al., 2008; Sangiorgi et al., 2008; Sluijs et al., 2008a; Sluijs et al., 2009). At ~371.2 mcd a drop in BIT index and a change in the palynological assemblages corresponds to an interval of greenish sediment, suggestive of pronounced amounts of glauconite. These changes are consistent with local relative sea level rise, causing a somewhat more distal position relative to the shoreline. However, the sediment remains dominantly siliciclastic and organic terrestrial components, particularly pollen and spores, remain abundant still indicating a shallow setting (Sluijs et al., 2008a; Sluijs et al., 2008b). Increased contributions of isoGDGTs produced at depth would be expected to have caused a systematic cold bias but based on linear regression analysis the large variability in GDGT-2/GDGT-3 ratios is unrelated to the recorded variability in TEX_{86} values. The

Deleted: where water depth is

Deleted: between 1 and

Deleted: from the bottom of the study section up to

Deleted: up

Deleted: values

Deleted: also highly

Deleted: averaging 7.4 and

Deleted: lthough

Deleted: support a change towards a

Deleted: at ~371.2 mcd, t

Moved down [1]: The high GDGT-2/GDGT-3 ratio values can therefore not be explained by contributions of deep dwelling archaea.

Deleted: deed, in

Deleted: . However,

Moved (insertion) [1]

high GDGT-2/GDGT-3 ratio values can therefore not be explained by contributions of deep dwelling archaea.

In a study of the last 160 kyr in the South China Sea, Dong et al. (2019) found that very high GDGT-2/GDGT-3 ratios (~9 but up to 13) correspond with high values in nitrogen isotope ratios, interpreted to reflect low contributions in diazotroph N_2 fixation and enhanced upwelling. In our record, the high GDGT-2/GDGT-3 ratios are associated with normal marine conditions and the dinocyst assemblages are not indicative of upwelling conditions (Sluijs et al., 2009). Unfortunately, the available nitrogen isotope record (Knies et al., 2008) does not cover this interval in sufficient resolution to assess a relation with diazotroph activity. The increase in GDGT-2/GDGT-3 ratio correlates to a strong drop in BIT index values and an increase in normal marine dinocyst species (Sluijs et al., 2009), but a shift to more open marine environment does not explain the high ratio values. As such, the cause of the high GDGT-2/GDGT-3 ratios in this interval remains unclear but we consider it highly unlikely to relate to contributions of deep dwelling Thaumarchaeota.

Deleted: ntriguingly, i

Deleted: s

Deleted: our study

Deleted: very

5.1.4 Oxygen concentrations and ammonium oxidation rates

A variety of non-thermal factors can impact TEX_{86} values, including ammonium and oxygen concentrations and growth phase (Elling et al., 2014; Qin et al., 2014; Hurley et al., 2016). Across the studied interval of the ACEX core, several intervals of seafloor and water column anoxia have been identified based on organic and inorganic proxies, notably during the PETM and ETM2 (Sluijs et al., 2006; Stein et al., 2006; Sluijs et al., 2008b; Sluijs et al., 2009; März et al., 2010).

Particularly suspect is an interval of low TEX_{86} values that marks the middle of the ETM2 interval, directly following a ~4 °C warming at its onset (Sluijs et al., 2009).

This interval is also marked by the presence of sulfur-bound isorenieratane (Sluijs et al., 2009), a derivative of isorenieratene. This biomarker is produced by the brown strain of green sulfur bacteria that require light for photosynthesis and free sulfide, indicating euxinic conditions in the (lower) photic zone (Sinninghe Damsté et al., 1993). We also record a concomitant shift in several methane-related indicators, GDGT-2/GDGT-3 ratio values and the ΔRI. A mid-ETM2 cooling signal has not been recorded at other study sites and this interval marks the occurrence of pollen of thermophilic plants such as palms and baobab (Sluijs et al., 2009; Willard et al., 2019). Therefore, the low TEX_{86} values were suggested to reflect thaumarcheotal depth migration to the deeper chemocline due to euxinic conditions (Sluijs et al., 2009), similar to the modern Black Sea (Coolen et al., 2007; Wakeham et al., 2007) and the Mediterranean Sea during sapropel formation (Menzel et al., 2006).

More recent work has indicated that the isolated marine Thaumarchaeotal species *Nitrosopumilus maritimus* produces lower TEX_{86} values with higher ammonia oxidation rates (Hurley et al., 2016) and O_2 concentrations (Qin et al., 2015). Although this observation is difficult to extrapolate to the total response of the Thaumarcheotal community in the marine environment on geological time scales, lower O_2 availability should lower oxidation rates leading to higher TEX_{86} values (Qin et al., 2015; Hurley et al., 2016). However, we record a drop in TEX_{86} values with the development of anoxia during ETM2. The nature of the anomalously low cyclization in the ETM2 isoGDGT assemblage, which passes all quality tests regarding GDGT distribution (Figure 6), remains therefore elusive.

Deleted: , a

Deleted: In general, however, if the relatively restricted and low-O_2 setting had any impact on TEX_{86} values, these culture studies (Qin et al., 2015; Hurley et al., 2016) suggest it would have led to an underestimate of the SST.

5.2 Origin and environmental forcing of brGMGTs

The relative abundances of brGMGTs in our samples are surprisingly high. On average, they comprise 25% of the total branched GDGT and GMGT assemblage. The limited literature on modern occurrences implies that both terrestrial and marine sources may have contributed to the brGMGT assemblage. Data from marine sediments (Liu et al., 2012) and the water column (Xie et al., 2014), clearly shows production within the marine realm. Their occurrence in modern peats (Naafs et al., 2018a), lake sediments (Baxter et al., 2019) and Paleogene lignites (Inglis et al., 2019) might also imply transport from land to marine sediments. A soil-derived source is currently unsupported, as they were most often below detection limit in recent studies of geothermally heated soils (De Jonge et al., 2019) and a soil transect from the Peruvian Andes (Kirkels et al., 2020). The brGMGT abundances we record are close to the maximum abundance found in modern peats (Naafs et al., 2018a). However, significant input of peat-derived organic matter into our study site is inconsistent with the low input of peat-derived *Sphagnum* spores (Willard et al., 2019). Alternatively, the high abundance of brGMGTs could also be related to subsurface production in marine sediments. An analogous process was invoked by Naafs et al. (2018a) to explain very high abundance of brGMGTs in an early Paleogene lignite. Collectively, however, we surmise that production in the marine realm may be an important contributor to the brGMGT pool in our setting.

Several factors may contribute to the rise in the abundance of brGMGTs relative to brGDGTs across the PETM. Higher relative abundances of brGMGTs in modern peats generally occur at higher mean annual air temperatures (Naafs et al., 2018a) and so this signal could relate to warming during the PETM if their origin at the study site is terrestrial. However, since we consider it likely that a large part of the brGMGTs

Deleted: the

Deleted: , which

Deleted: argue

assemblage is of marine origin, the rise in brGMGT abundance likely relates to the previously recorded (Sluijs et al., 2006; Sluijs et al., 2008b) sea level rise during the PETM at the study site. This is consistent with the increase in marine brGMGT production relative to terrestrial brGDGT supply to the study site (Figure 7b). This is consistent with the inverse correlation between brGMGT abundance and the BIT index (Figure 7b). Lastly, if the production of marine brGMGTs was focused in oxygen minimum zones (Xie et al., 2014), the development of low oxygen conditions in the water column based on several indicators, such as the presence of isorenieratane (Sluijs et al., 2006), might have increased the production of brGMGTs in the water column. It is also possible that all of these factors contributed to the changes in abundance of brGMGTs relative to brGDGTs across the PETM.

The brGMGT-I proxy does not produce temperature trends similar to those seen in TEX_{86} or MBT'_{5me} (Figure 7d). If the majority of the brGMGTs are of marine origin, this indicates that brGMGTs produced in the marine realm do not respond to temperature as was hypothesized based on the African Lake dataset by Baxter et al. (2019).

Also the application of the $H\text{-}MBT_{acyclic}$ index (equation 7) appeared problematic because, similar to Baxter et al. (2019), we identified several more isomers than Naafs et al. (2018a, who developed this index) detected in their peat samples. It therefore remains unclear which of our peaks should be used to calculate the $H\text{-}MBT_{acyclic}$ index values. We therefore show the two plausible options. For the first, we use all peaks with *m/z* 1020, 1034 and 1048 (*H-MBT-all* in Figure 7e) within the expected retention time window. However, based on our chromatography, we consider it more likely that the dominant peaks identified by Naafs et al. (2018a) at *m/z* 1020 and 1034 represent H1020c and H1034b, respectively, and therefore use only those in addition to the single

Deleted: . If so

Deleted: , causing an

Deleted: e

Deleted: is

Deleted: different

identifiable peak at *m/z* 1048 as a second option (H-*MBT* (H1020*c*, *H1034*) in Figure 7e. Both options show a clear rise across the PETM, although the HMBT (H1020c, H1034a) shows a larger signal and somewhat better correspondence in absolute values to $MBT_{acyclic}$, though with more scatter. A close correspondence between MBT*acyclic* and HMBT has also been found in a lignite that has been assigned to the PETM (Inglis et al., 2019).

If the dominant source of the brGMGTs was marine throughout the record, the increase in methylation possibly relates to warming. This would not be unprecedented as marine-produced brGDGTs show an increase in methylation as a function of temperature (Dearing Crampton-Flood et al., 2018). Sollic et al. (2017) also suggest that archaeal-derived isoprenoid GMGTs produced in marine sediments incorporate additional methyl groups at higher sediment temperatures. Water column oxygen concentrations and pH also changed at our site during the PETM, which potentially affected distributions. Extensive evaluation of brGMGT distributions in modern samples is therefore required to assess the proxy potential.

5.3 Uncertainty on TEX_{86}-based SST estimates.

5.3.1 Uncertainty based on calibration dataset

To calculate SSTs, we use 1) the BAYSPAR method (Tierney and Tingley, 2014), which assumes a linear relationship between TEX_{86} and SST, and 2) TEX_{86}^{H} (Kim et al., 2010), which assumes a non-linear relationship between TEX_{86} and SST. Differences between these calibrations are smaller than the calibration errors (Figure 6) because the TEX_{86} values in the ACEX dataset all fall within the range of the modern core top calibration. Taken together, both indices imply that mean annual SSTs varied

Deleted: was
Deleted: recent analysis of a
Deleted: seems to correspond
Deleted: ,
Deleted: although interestingly, no apparent relation with temperature was found
Deleted: If a pronounced part of brGMGTs within the terrestrially-dominated Paleocene part of the section is of terrestrial origin, it is possible that the drop in the relative contribution of terrestrially-derived versus marine brGMGTs influenced these records. However, i
Deleted: , and
Deleted: also
Deleted:
Deleted: {Sollich, 2017 #2025}
Deleted: However, along with the unresolved brGMGT sourcing, during the PETM at the study site also w
Deleted: –
Deleted: -
Deleted:
Deleted: –
Deleted: well
Deleted: Collectively, t
Deleted: at face value
Deleted: the data

between 18 °C and 28 °C in the early Eocene, providing strong evidence for remarkable early Eocene warmth in the Arctic region.

The TEX_{86}^{H} calibration has a calibration error of 2.5 °C (residual mean standard error; RSME) (Kim et al., 2010). The BAYSPAR method yields possible values that range ~6 °C from the most probable value (Figure 6), but these uncertainty estimates are more comparable than is immediately apparent, as this analysis takes a 90% confidence interval compared to the 68% probability of RSME. All of the calibrations and methods to obtain values and uncertainties are based on a modern core-top dataset and thus implicitly include potential confounding factors such as seasonality and depth of production and export. However, there is no (quantitative) constraint on any of these parameters in the calibration data set. This is particularly important for the studied region because it represents a polar endmember of the marine environment with highly seasonal production and export and potentially high seasonality in temperature. In the modern ocean, relations between SST and TEX_{86} in the Arctic and ice-proximal Southern Ocean settings differ from the global ocean. This is attributed to a change in viscoelastic adaptation to temperature at the low end and/or a change in the Thaumarchaeotal community (Kim et al., 2010; Ho et al., 2014; Tierney and Tingley, 2014). This may mask potential confounding factors that may be relevant specifically to polar environments. This is important here, where the polar regions were ice free and the functioning of physical, chemical and biological ocean systems were fundamentally different from present day. This uncertainty is not accounted for using traditional regression analyses or Bayesian techniques and quantification of uncertainty in non-analogue climates remains extremely difficult.

Deleted: implies

Deleted: However, a

Deleted: ,

Deleted: for our case, a situation in which

Deleted: implies that any

Deleted: calculated based on the modern database, regardless whether it is done based on

Deleted: BAYSPAR, has no direct value for determination of uncertainty in our case because the caveats and confounding factors do not influence uncertainty in the same way in the Eocene as in the modern. Q

Deleted: is at this point, therefore, *5.3.2 Constraints from independent proxy data*

Independent proxy data may provide additional constraints. The appearance of the dinoflagellate cyst genus *Apectodinium* during the PETM and ETM2 in the Arctic basin (Sluijs et al., 2006; Sluijs et al., 2009; Harding et al., 2011) provide qualitative support for pronounced warming and apparent subtropical conditions. Recent efforts to quantify the paleoecological affinities of this now extinct genus have suggested a required minimum temperature of ~20°C (Frieling et al., 2014; Frieling and Sluijs, 2018). Although this value is partly based on TEX_{86} data from the ACEX cores, it is supported by data from an epicontinental site in Siberia (Frieling et al., 2014).

A second line of independent proxy evidence includes vegetation reconstructions. As indicated above, the TEX_{86} results are qualitatively consistent with the ample evidence for thermophilic plants and animals in the Arctic (e.g., Heer, 1869; Schweitzer, 1980; Greenwood and Wing, 1995; Uhl et al., 2007; Suan et al., 2017). Particularly valuable are minimum winter temperature tolerances for specific plant species. Palynological analyses have indicated the presence of palm and baobab pollen within the PETM and ETM2 intervals in the ACEX cores (Sluijs et al., 2009; Willard et al., 2019). Modern palms are unable to tolerate sustained intervals of frost and sexual reproduction is limited to regions where the coldest month mean temperature (CMMT) is significantly above freezing (Van der Burgh, 1984; Greenwood and Wing, 1995). This threshold was was recently quantified to be ≥ 5.2 °C (Reichgelt et al., 2018). The presence of baobab within the PETM interval and ETM2 also indicate mean winter air temperatures of at least 6 °C (Willard et al., 2019). Importantly, these plants were not encountered in the intervals outside the PETM and ETM2, suggesting background coldest month mean air temperatures were potentially too low (<6ºC) to support megathermal vegetation.

Deleted: whilst

Deleted: The latter

Deleted: support

Deleted: these

Deleted: elements

Pollen of palms and *Avicennia* mangroves were recently identified in time-equivalent sections in Arctic Siberia (Suan et al., 2017). Although the details of stratigraphic framework for these records may be somewhat problematic, these findings indicate elevated CMMT estimates on land (>5.5 °C) and in the surface ocean (>13 °C) during the late Paleocene and early Eocene (Suan et al., 2017).

Apparently conflicting evidence comes from the occurrence of glendonites and erratics in specific stratigraphic levels in Paleocene and Eocene strata in Spitsbergen, interpreted to reflect 'cold snaps' in climate (Spielhagen and Tripati, 2009). Some of these stratigraphic levels are very close to (or even potentially within) the PETM, considering the local stratigraphic level of the PETM (Cui et al., 2011; Harding et al., 2011). However, glendonites and erratics have not been found at the exact same stratigraphic levels as thermophilic biota (Spielhagen and Tripati, 2009). The formation and stability of ikaite (the precursor mineral of the diagenetic glendonites) in Spitsbergen was dependent on relatively low temperature, arguably persistent near-freezing sea water temperatures in the sediment (Spielhagen and Tripati, 2009). However, glendonite occurrences in other settings (e.g. Mesozoic sediments in mid-latitude regions, Teichert and Luppold, 2013) have recently also been linked to methane seeps (Morales et al., 2017). Therefore, the specific temperature constraints implied by glendonites under such conditions are subject of debate. Future work should apply temperature reconstructions based on the geochemical composition of the glendonites, and biomarkers or biota on corresponding strata to assess whether glendonite occurrence is related to colder climates.

The estimate on seasonal minima provides an important constraint on Arctic climatology during the PETM and ETM2. Most likely, the palms and baobabs grew close to the shore, where the relative heat of the ocean kept atmospheric temperatures

Deleted: context

Deleted: of

Deleted: provide good evidence for very high coldest month mean temperatures, both air

Deleted: and SST

Deleted: , although

Deleted: Clearly, however, the glendonite occurrences may imply episodes of colder climates and follow up

Deleted: proxy consistency

Deleted: is

relatively high during the winter. If minimum winter SSTs were in the range of the SST reconstructions based on the nearby *Avicennia* mangrove pollen (Suan et al., 2017), which for open ocean settings would perhaps amount to ~10 °C, then summer SST must have soared to at least 30 °C in summer if TEX_{86}–based SST reconstructions of ~20 °C truly reflects the annual mean. It would imply an SST seasonality of ~20 °C, much higher than any modern open marine setting. In the present day Arctic Ocean, heat is seasonally stored and released in sea ice melting and freezing, and sea ice cover insulates the ocean and reflects much sunlight, resulting in a seasonal cycle of not more than 1.5 °C, even in ice-free regions (Chepurin and Carton, 2012). However, coupled model simulations have indicated that the future loss of sea ice will greatly enhance the seasonal SST range to up to 10 °C in 2300 given unabated CO_2 emissions (Carton et al., 2015). With year-round snow and ice-free conditions, even stronger summer stratification during the Eocene due to higher greenhouse gas concentrations and fresh-water supply through an enhanced hydrological cycle (Pierrehumbert, 2002; Carmichael et al., 2017), a near-shore 20 °C seasonal cycle in Arctic Ocean SST may not be unrealistic, although it remains inconsistent with current-generation fully coupled, relatively low resolution, model simulations (e.g., Frieling et al., 2017).

Constraints from the total pollen assemblages in the ACEX cores based on a nearest living relative approach suggest Arctic mean annual temperatures on land of 13-18 °C, and summer temperatures significantly exceeding 20 °C during the PETM and ETM2 (Willard et al., 2019). Although these estimates come with much larger uncertainty than winter temperatures and may suffer from the non-analogous setting, they are generally lower than our TEX_{86} values. The brGDGT-based paleothermometer MBT'_{5me} (De Jonge et al., 2014) also indicates lower mean annual air temperatures than reported from TEX_{86} (Willard et al., 2019, Figure 7). These data, derived from the same UHPLC/MS

Deleted: , let alone the Arctic Ocean

Deleted: Also t

Deleted: temperatures

analyses as the isoGDGT data presented here, indicate mean annual air temperatures averaging ~18 °C during the PETM, with a residual mean calibration error of 4.8 °C. This value is ~7 °C lower than earlier estimates based on a slightly different method, analytical procedure and a smaller modern calibration dataset (Weijers et al., 2007a).

5.4 State of constraints on Paleocene-Eocene Arctic temperatures

To unlock the unique premise of Eocene climates for testing the skill of current-generation fully coupled climate models under high greenhouse gas forcing, proxy data and models are ideally approached separately. Among the most important implications of the Arctic temperature estimates are reconstructions of the meridional temperature gradients. Importantly, not a single simulation using an IPCC-class model of early Paleogene climate has produced Arctic annual mean sea surface temperatures close to the ACEX TEX_{86}-based reconstructions without unrealistically high tropical SSTs (Lunt et al., 2012). Recent simulations using the Community Earth System Model (CESM) versions 1 (Frieling et al., 2017; Cramwinckel et al., 2018) and 1.2 (Zhu et al., 2019) using Eocene boundary conditions produced climates that correspond to SST reconstructions in many ocean regions based on several proxies, but still produced cooler mean annual SSTs for the Arctic Ocean than suggested by TEX_{86} (Frieling et al., 2017; Cramwinckel et al., 2018; Zhu et al., 2019). TEX_{86} also indicates SSTs higher than in these model simulations at several sites along the Antarctic margin (Bijl et al., 2009; Bijl et al., 2013). The question thus remains if the conversion of TEX_{86} values towards mean annual SST using any modern core-top calibration for high latitude Paleogene locations is valid, or if the climate models still significantly underestimate polar temperatures. Certainly, if interpreted as mean annual SST, TEX_{86}-based

Deleted: (CESM-1)

estimates are high compared to the few available additional estimates, notably based on vegetation, but the latter also suffer from similar uncertainties (e.g., Hollis et al., 2019). A few biases might lead to underestimates of meridional temperature gradients as indicated from TEX_{86}. First, the flat Eocene temperature gradient implied by TEX_{86} was suggested to result from erroneously calibrating the proxy to SST rather than to the temperature of the subsurface (Ho and Laepple, 2016). The rationale is that the meridional temperature gradient is smaller in deeper waters than it is in the surface. However, the idea was contested for multiple reasons, including the fact that sediments at most Eocene study sites, such as the ACEX site, were deposited at a depth of less than 200m, making the application of a deep subsurface (>1000m) calibration inappropriate (Tierney et al., 2017). Moreover, recent analyses have indicated that the TEX_{86} signal dominantly reflects temperature of top 200 m of the water column (Zhang and Liu, 2018).

Deleted: exaggerate

Secondly, as suggested previously (Sluijs et al., 2006), if TEX_{86} were biased towards any season in the non-analogue Arctic Ocean, it would be the summer, the dominant season of organic matter export towards the seafloor through fecal pelleting or marine snow aggregates. Vegetation suggests very high winter continental coldest month mean air temperatures of at least 6-8 °C (Sluijs et al., 2009; Suan et al., 2017; Willard et al., 2019), coastal coldest month mean SSTs of >13 °C (Suan et al., 2017), and terrestrial mean annual and warmest month mean temperature on land of 13-21 °C and >20°C, respectively (Suan et al., 2017; Willard et al., 2019) (see section 5.3.2). These estimates are closer to the most recent model simulations and lower than the existing TEX_{86} (e.g., Frieling et al., 2017; Zhu et al., 2019). If TEX_{86}-implied SST of ~25 °C is skewed towards a summer estimate, this would decrease the model-data bias regarding the meridional temperature gradient estimates. Given the current uncertainties in the use of

TEX_{86} for the non-analogue Arctic Ocean, we however cannot independently constrain this.

6. Conclusions

We analyzed isoGDGT and brGMGT (H-shaped brGDGT) distributions in sediments recovered from the Paleocene-Eocene Thermal Maximum (PETM; ~56 Ma) to Eocene Thermal Maximum 2 (ETM2; ~54 Ma) interval on Lomonosov Ridge, Arctic Ocean using state-of-the-art analytical procedures, compare them to the original dataset (Sluijs et al., 2006; Sluijs et al., 2009) and interpret the results following the currently available TEX_{86} proxy constraints.

Deleted: anched

Although contributions of isoGDGTs from land complicate TEX_{86} paleothermometry in some stratigraphic intervals, temperature was the dominant variable controlling TEX_{86} values. Background early Eocene SSTs exceed ~20 °C and peak warmth occurred during the PETM and ETM2. However, uncertainty estimates of these SSTs based on the non-analogue modern ocean, remains complex. Temperature constraints from terrestrial vegetation support remarkable warmth in the study section and elsewhere in the Arctic basin, notably coldest month mean temperatures around 10 °C at least within the PETM and ETM2. If TEX_{86}-derived SSTs of ~20 °C truly represent mean annual SSTs, the seasonal range of Arctic SST might have been in the order of 20 °C. If SST estimates are entirely skewed towards the summer season, seasonal ranges in the order of 10 °C may be considered comparable to those simulated in future ice-free Arctic Ocean scenarios.

We find abundant brGMGTs, which appear predominantly produced in the marine realm at the study site. Their abundance increases during the PETM, likely due to sea level rise and perhaps due to warming and a drop in seawater oxygen concentrations.

Although speculative, an increase in brGMGT methylation during the PETM may be a function of temperature, but a relation between brGMGT distribution and environmental parameters including temperature is yet to be confirmed.

6. Data Availability

All data is provided in the Supplement Table and will be included in the PANGAEA database upon publication of this paper.

7. Sample Availability

Requests for materials can be addressed to A.Sluijs@uu.nl

8. Author Contributions

AS initiated the study, KGJN generated the data, JF modeled terrestrial contributions of isoGDGTs based on published information and the new Crenarchaeol data of the modern peat dataset, which was contributed by GNI. All authors contributed to the interpretation of the data and AS wrote the paper with input from all authors.

9. Competing Interests

The authors declare no competing interests

10. Acknowledgments

We thank the ACEX scientific party for collaborations over the past 16 years, the International Ocean Discovery Program (IODP) for access to ACEX samples and data, and the Dutch Research Council (NWO) for their continued support to IODP. We thank Linda van Roij for analytical support.

This research was funded by European Research Council Consolidator Grant 771497 awarded to AS and the Netherlands Earth System Science Centre, funded through a Gravitation Grant by the Netherlands Ministry of Education, Culture and Science and NWO. GNI acknowledges a GCRF Royal Society Dorothy Hodgkin Fellowship and thanks David Naafs for providing the original chromatograms published in Naafs et al. (2018b).

Deleted: .

11. References

Backman, J., Moran, K., McInroy, D. B., Mayer, L. A., and Expedition-302-Scientists: Proceedings of the Integrated Ocean Drilling Program, 302, Integrated Ocean Drilling Program Management International, Inc., Edinburgh, 2006.

Baxter, A. J., Hopmans, E. C., Russell, J. M., and Sinninghe Damsté, J. S.: Bacterial GMGTs in East African lake sediments: Their potential as palaeotemperature indicators, Geochim Cosmochim Ac, 259, 155-169, https://doi.org/10.1016/j.gca.2019.05.039, 2019.

Deleted: Barke, J., Abels, H. A., Sangiorgi, F., Greenwood, D. R., Sweet, A. R., Donders, T., Reichart, G.-J., Lotter, A. F., and Brinkhuis, H.: Orbitally forced Azolla blooms and Middle Eocene Arctic hydrology: Clues from palynology, Geology, 39, 427-430, 10.1130/G31640.1, 2011.¶
Barke, J., van der Burgh, J., van Konijnenburg-van Cittert, J. H. A., Collinson, M. E., Pearce, M. A., Bujak, J., Heilmann-Clausen, C., Speelman, E. N., van Kempen, M. M. L., Reichart, G.-J., Lotter, A. F., and Brinkhuis, H.: Coeval Eocene blooms of the freshwater fern Azolla in and around Arctic and Nordic seas, Palaeogeography, Palaeoclimatology, Palaeoecology, 337-338, 108-119, https://doi.org/10.1016/j.palaeo.2012.04.002, 2012.¶

Berry, E. W.: A Possible Explanation of Upper Eocene Climates, Proceedings of the American Philosophical Society, 61, 1-14, 1922.

Besseling, M. A., Hopmans, E. C., Bale, N. J., Schouten, S., Damsté, J. S. S., and Villanueva, L.: The absence of intact polar lipid-derived GDGTs in marine waters dominated by Marine Group II: Implications for lipid biosynthesis in Archaea, Scientific Reports, 10, 294, 10.1038/s41598-019-57035-0, 2020.

Bijl, P. K., Schouten, S., Sluijs, A., Reichart, G.-J., Zachos, J. C., and Brinkhuis, H.: Early Palaeogene temperature evolution of the southwest Pacific Ocean, Nature, 461, 776-779, 2009.

Bijl, P. K., Bendle, J. A. P., Bohaty, S. M., Pross, J., Schouten, S., Tauxe, L., Stickley, C. E., McKay, R. M., Rohl, U., Olney, M., Sluijs, A., Escutia, C., Brinkhuis, H., and the Expedition 318 Scientists: Eocene cooling linked to early flow across the Tasmanian Gateway, Proceedings of the National Academy of Sciences, 110, 9645-9650, 10.1073/pnas.1220872110, 2013.

Blaga, C. I., Reichart, G.-J., Heiri, O., and Sinninghe Damsté, J. S.: Tetraether membrane lipid distributions in water-column particulate matter and sediments: a study of 47 European lakes along a north–south transect, Journal of Paleolimnology, 41, 523-540, 10.1007/s10933-008-9242-2, 2009.

Deleted: Brinkhuis, H., Schouten, S., Collinson, M. E., Sluijs, A., Sinninghe Damsté, J. S., Dickens, G. R., Huber, M., Cronin, T. M., Onodera, J., Takahashi, K., Bujak, J. P., Stein, R., van der Burgh, J., Eldrett, J. S., Harding, I. C., Lotter, A. F., Sangiorgi, F., van Konijnenburg-van Cittert, H., de Leeuw, J. W., Matthiessen, J., Backman, J., Moran, K., and the Expedition 302 Scientists: Episodic fresh surface waters in the Eocene Arctic Ocean, Nature, 441, 606-609, 2006.¶

Carton, J. A., Ding, Y., and Arrigo, K. R.: The seasonal cycle of the Arctic Ocean under climate change, Geophysical Research Letters, 42, 7681-7686, doi:10.1002/2015GL064514, 2015.

Chepurin, G. A., and Carton, J. A.: Subarctic and Arctic sea surface temperature and its relation to ocean heat content 1982–2010, Journal of Geophysical Research: Oceans, 117, doi:10.1029/2011JC007770, 2012.

Coolen, M. J. L., Abbas, B., Bleijswijk, J. v., Hopmans, E. C., Kuypers, M. M. M., Wakeham, S. G., and Damsté, J. S. S.: Putative ammonia-oxidizing Crenarchaeota in suboxic waters of the Black Sea: a basin-wide ecological study using 16S ribosomal and functional genes and membrane lipids, Environ Microbiol, 9, 1001-1016, 2007.

Cramwinckel, M. J., Huber, M., Kocken, I. J., Agnini, C., Bijl, P. K., Bohaty, S. M., Frieling, J., Goldner, A., Hilgen, F. J., Kip, E. L., Peterse, F., van der Ploeg, R., Röhl, U., Schouten, S., and Sluijs, A.: Synchronous tropical and polar temperature evolution in the Eocene, Nature, 559, 382-386, 10.1038/s41586-018-0272-2, 2018.

Cui, Y., Kump, L. R., Ridgwell, A. J., Charles, A. J., Junium, C. K., Diefendorf, A. F., Freeman, K. H., Urban, N. M., and Harding, I. C.: Slow release of fossil carbon during the Palaeocene-Eocene Thermal Maximum, Nature Geoscience, 4, 481-485, 2011.

Dawson, M. R., West, R. M., Langston Jr, W., and Hutchison, J. H.: Paleogene terrestrial vertebrates: Northernmost occurrence, Ellesmere Island, Canada, Science, 192, 781-782, 1976.

De Jonge, C., Hopmans, E. C., Zell, C. I., Kim, J.-H., Schouten, S., and Sinninghe Damsté, J. S.: Occurrence and abundance of 6-methyl branched glycerol dialkyl glycerol tetraethers in soils: Implications for palaeoclimate reconstruction, Geochim Cosmochim Ac, 141, 97-112, https://doi.org/10.1016/j.gca.2014.06.013, 2014.

De Jonge, C., Radujković, D., Sigurdsson, B. D., Weedon, J. T., Janssens, I., and Peterse, F.: Lipid biomarker temperature proxy responds to abrupt shift in the bacterial community composition in geothermally heated soils, Org Geochem, 137, 103897, https://doi.org/10.1016/j.orggeochem.2019.07.006, 2019.

De Rosa, M., Esposito, E., Gambacorta, A., Nicolaus, B., and Bu'Lock, J. D.: Effects of temperature on ether lipid composition of Caldariella acidophila, Phytochemistry, 19, 827-831, https://doi.org/10.1016/0031-9422(80)85120-X, 1980.

Dearing Crampton-Flood, E., Peterse, F., Munsterman, D., and Sinninghe Damsté, J. S.: Using tetraether lipids archived in North Sea Basin sediments to extract North Western European Pliocene continental air temperatures, Earth and Planetary Science Letters, 490, 193-205, https://doi.org/10.1016/j.epsl.2018.03.030, 2018.

Dong, L., Li, Z., and Jia, G.: Archaeal ammonia oxidation plays a part in late Quaternary nitrogen cycling in the South China Sea, Earth and Planetary Science Letters, 509, 38-46, https://doi.org/10.1016/j.epsl.2018.12.023, 2019.

Douglas, P. M. J., Affek, H. P., Ivany, L. C., Houben, A. J. P., Sijp, W. P., Sluijs, A., Schouten, S., and Pagani, M.: Pronounced zonal heterogeneity in Eocene southern high-latitude sea surface temperatures, Proceedings of the National Academy of Sciences of the United States of America, 111, 6582-6587, 2014.

Eberle, J. J., and Greenwood, D. R.: Life at the top of the greenhouse Eocene world—A review of the Eocene flora and vertebrate fauna from Canada's High Arctic, GSA Bulletin, 124, 3-23, 10.1130/B30571.1, 2012.

Elling, F. J., Könneke, M., Lipp, J. S., Becker, K. W., Gagen, E. J., and Hinrichs, K.-U.: Effects of growth phase on the membrane lipid composition of the thaumarchaeon Nitrosopumilus maritimus and their implications for archaeal lipid distributions in the marine environment, Geochim Cosmochim Ac, 141, 579-597, https://doi.org/10.1016/j.gca.2014.07.005, 2014.

Elling, F. J., Könneke, M., Mußmann, M., Greve, A., and Hinrichs, K.-U.: Influence of temperature, pH, and salinity on membrane lipid composition and TEX86 of marine planktonic thaumarchaeal isolates, Geochim Cosmochim Ac, 171, 238-255, https://doi.org/10.1016/j.gca.2015.09.004, 2015.

Estes, R., and Hutchinson, J. H.: Eocene Lower Vertebrates from Ellesmere Island, Canadian Arctic Archipelago, Palaeogeography, Palaeoclimatology, Palaeoecology, 30, 325-347, 1980.
Evans, D., Sagoo, N., Renema, W., Cotton, L. J., Müller, W., Todd, J. A., Saraswati, P. K., Stassen, P., Ziegler, M., Pearson, P. N., Valdes, P. J., and Affek, H. P.: Eocene greenhouse climate revealed by coupled clumped isotope-Mg/Ca thermometry, Proceedings of the National Academy of Sciences, 115, 1174-1179, 10.1073/pnas.1714744115, 2018.
Frieling, J., Iakovleva, A. I., Reichart, G. J., Aleksandrova, G. N., Gnibidenko, Z. N., Schouten, S., and Sluijs, A.: Paleocene-Eocene warming and biotic response in the epicontinental West Siberian Sea, Geology, 42, 767-770, 2014.
Frieling, J., Gebhardt, H., Huber, M., Adekeye, O. A., Akande, S. O., Reichart, G.-J., Middelburg, J. J., Schouten, S., and Sluijs, A.: Extreme warmth and heat-stressed plankton in the tropics during the Paleocene-Eocene Thermal Maximum, Science Advances, 3, e1600891, 10.1126/sciadv.1600891, 2017.
Frieling, J., and Sluijs, A.: Towards quantitative environmental reconstructions from ancient non-analogue microfossil assemblages: Ecological preferences of Paleocene – Eocene dinoflagellates, Earth-Science Reviews, 185, 956-973, https://doi.org/10.1016/j.earscirev.2018.08.014, 2018.
Greenwood, D. R., and Wing, S. L.: Eocene continental climates and latitudinal temperature gradients, Geology, 23, 1044-1048, 1995.
Greenwood, D. R., Basinger, J. F., and Smith, R. Y.: How wet was the Arctic Eocene rain forest? Estimates of precipitation from Paleogene Arctic macrofloras, Geology, 38, 15-18, 10.1130/G30218.1, 2010.
Harding, I. C., Charles, A. J., Marshall, J. E. A., Pälike, H., Roberts, A. P., Wilson, P. A., Jarvis, E., Thorne, R., Morris, E., Moremon, R., Pearce, R. B., and Akbari, S.: Sea-level and salinity fluctuations during the Paleocene-Eocene thermal maximum in Arctic Spitsbergen, Earth and Planetary Science Letters, 303, 97-107, 2011.
Heer, O.: Flora fossilis Arctica, Kongliga Swenska Wetenskaps Academiens Handlingar, 4, Stockholm, Sweden, 41 pp., 1869.
Ho, S. L., Mollenhauer, G., Fietz, S., Martínez-Garcia, A., Lamy, F., Rueda, G., Schipper, K., Méheust, M., Rosell-Melé, A., Stein, R., and Tiedemann, R.: Appraisal of TEX86 and TEX86L thermometries in subpolar and polar regions, Geochim Cosmochim Ac, 131, 213-226, https://doi.org/10.1016/j.gca.2014.01.001, 2014.
Ho, S. L., and Laepple, T.: Flat meridional temperature gradient in the early Eocene in the subsurface rather than surface ocean, Nature Geoscience, 9, 606-610, 10.1038/ngeo2763.http://www.nature.com/ngeo/journal/v9/n8/abs/ngeo2763.html #supplementary-information, 2016.
Hollis, C. J., Dunkley Jones, T., Anagnostou, E., Bijl, P. K., Cramwinckel, M. J., Cui, Y., Dickens, G. R., Edgar, K. M., Eley, Y., Evans, D., Foster, G. L., Frieling, J., Inglis, G. N., Kennedy, E. M., Kozdon, R., Lauretano, V., Lear, C. H., Littler, K., Lourens, L., Meckler, A. N., Naafs, B. D. A., Pälike, H., Pancost, R. D., Pearson, P. N., Röhl, U., Royer, D. L., Salzmann, U., Schubert, B. A., Seebeck, H., Sluijs, A., Speijer, R. P., Stassen, P., Tierney, J., Tripati, A., Wade, B., Westerhold, T., Witkowski, C., Zachos, J. C., Zhang, Y. G., Huber, M., and Lunt, D. J.: The DeepMIP contribution to PMIP4: methodologies for selection, compilation and analysis of latest Paleocene and early Eocene climate proxy data, incorporating version 0.1 of the DeepMIP database, Geosci. Model Dev., 12, 3149-3206, 10.5194/gmd-12-3149-2019, 2019.

Hopmans, E. C., Schouten, S., Pancost, R. D., Meer, M. T. J. v. d., and Damsté, J. S. S.: Analysis of intact tetraether lipids in archaeal cell material and sediments by high performance liquid chromatography/atmospheric pressure chemical ionization mass spectrometry, Rapid Communications in Mass Spectrometry, 14, 585-589, 2000.

Hopmans, E. C., Weijers, J. W. H., Schefuß, E., Herfort, L., Sinninghe Damsté, J. S., and Schouten, S.: A novel proxy for terrestrial organic matter in sediments based on branched and isoprenoid tetraether lipids, Earth and Planetary Science Letters, 224, 107-116, 2004.

Hopmans, E. C., Schouten, S., and Sinninghe Damsté, J. S.: The effect of improved chromatography on GDGT-based palaeoproxies, Org Geochem, 93, 1-6, https://doi.org/10.1016/j.orggeochem.2015.12.006, 2016.

Hurley, S. J., Elling, F. J., Könneke, M., Buchwald, C., Wankel, S. D., Santoro, A. E., Lipp, J. S., Hinrichs, K.-U., and Pearson, A.: Influence of ammonia oxidation rate on thaumarchaeal lipid composition and the TEX_{86} temperature proxy, Proceedings of the National Academy of Sciences, 113, 7762-7767, 10.1073/pnas.1518534113, 2016.

Inglis, G. N., Farnsworth, A., Lunt, D., Foster, G. L., Hollis, C. J., Pagani, M., Jardine, P. E., Pearson, P. N., Markwick, P., Galsworthy, A. M. J., Raynham, L., Taylor, K. W. R., and Pancost, R. D.: Descent toward the Icehouse: Eocene sea surface cooling inferred from GDGT distributions, Paleoceanography, 30, 1000-1020, 10.1002/2014PA002723, 2015.

Inglis, G. N., Farnsworth, A., Collinson, M. E., Carmichael, M. J., Naafs, B. D. A., Lunt, D. J., Valdes, P. J., and Pancost, R. D.: Terrestrial environmental change across the onset of the PETM and the associated impact on biomarker proxies: A cautionary tale, Global and Planetary Change, 181, 102991, https://doi.org/10.1016/j.gloplacha.2019.102991, 2019.

Jaeschke, A., Jørgensen, S. L., Bernasconi, S. M., Pedersen, R. B., Thorseth, I. H., and Früh-Green, G. L.: Microbial diversity of Loki's Castle black smokers at the Arctic Mid-Ocean Ridge, Geobiology, 10, 548-561, 10.1111/gbi.12009, 2012

Karner, M. B., DeLong, E. F., and Karl, D. M.: Archaeal dominance in the mesopelagic zone of the Pacific Ocean, Nature, 409, 507-510, 10.1038/35054051, 2001.

Kim, J.-H., Schouten, S., Hopmans, E. C., Donner, B., and Sinninghe Damste, J. S.: Global sediment core-top calibration of the TEX86 paleothermometer in the ocean, Geochim Cosmochim Ac, 72, 1154-1173, 2008.

Kim, J.-H., van der Meer, J., Schouten, S., Helmke, P., Willmott, V., Sangiorgi, F., Koç, N., Hopmans, E. C., and Sinninghe Damsté, J. S.: New indices and calibrations derived from the distribution of crenarchaeal isoprenoid tetraether lipids: Implications for past sea surface temperature reconstructions, Geochim Cosmochim Ac, 74, 4639-4654, 2010.

Kim, J.-H., Schouten, S., Rodrigo-Gámiz, M., Rampen, S., Marino, G., Huguet, C., Helmke, P., Buscail, R., Hopmans, E. C., Pross, J., Sangiorgi, F., Middelburg, J. B. M., and Sinninghe Damsté, J. S.: Influence of deep-water derived isoprenoid tetraether lipids on the paleothermometer in the Mediterranean Sea, Geochim Cosmochim Ac, 150, 125-141, http://dx.doi.org/10.1016/j.gca.2014.11.017, 2015.

Kirkels, F. M. S. A., Ponton, C., Galy, V., West, A. J., Feakins, S. J., and Peterse, F.: From Andes to Amazon: Assessing Branched Tetraether Lipids as Tracers for Soil Organic Carbon in the Madre de Dios River System, Journal of Geophysical Research: Biogeosciences, 125, e2019JG005270, 10.1029/2019jg005270, 2020.

Knies, J., Mann, U., Popp, B. N., Stein, R., and Brumsack, H.-J.: Surface water productivity and paleoceanographic implications in the Cenozoic Arctic Ocean, Paleoceanography, 23, PA1S16, 10.1029/2007pa001455, 2008.

Könneke, M., Bernhard, A. E., de la Torre, J. R., Walker, C. B., Waterbury, J. B., and Stahl, D. A.: Isolation of an autotrophic ammonia-oxidizing marine archaeon, Nature, 437, 543-546, 10.1038/nature03911, 2005.

Liu, X.-L., Summons, R. E., and Hinrichs, K.-U.: Extending the known range of glycerol ether lipids in the environment: structural assignments based on tandem mass spectral fragmentation patterns, Rapid Communications in Mass Spectrometry, 26, 2295-2302, 10.1002/rcm.6355, 2012.

Liu, Z., Pagani, M., Zinniker, D., DeConto, R., Huber, M., Brinkhuis, H., Shah, S. R., Leckie, R. M., and Pearson, A.: Global Cooling During the Eocene-Oligocene Climate Transition, Science, 323, 1187-1190, 10.1126/science.1166368, 2009.

Lunt, D. J., Jones, T. D., Heinemann, M., Huber, M., LeGrande, A., Winguth, A., Loptson, C., Marotzke, J., Roberts, C. D., Tindall, J., Valdes, P., and Winguth, C.: A model–data comparison for a multi-model ensemble of early Eocene atmosphere–ocean simulations: EoMIP, Climate of the Past, 8, 1717-1736, 2012.

März, C., Schnetger, B., and Brumsack, H. J.: Paleoenvironmental implications of Cenozoic sediments from the central Arctic Ocean (IODP Expedition 302) using inorganic geochemistry, Paleoceanography, 25, PA3206, 10.1029/2009pa001860, 2010.

Menzel, D., Hopmans, E. C., Schouten, S., and Sinninghe Damsté, J. S.: Membrane tetraether lipids of planktonic Crenarchaeota in Pliocene sapropels of the eastern Mediterranean Sea, Palaeogeography, Palaeoclimatology, Palaeoecology, 239, 1-15, 2006.

Mollenhauer, G., Basse, A., Kim, J.-H., Sinninghe Damsté, J. S., and Fischer, G.: A four-year record of UK′ 37- and TEX86-derived sea surface temperature estimates from sinking particles in the filamentous upwelling region off Cape Blanc, Mauritania, Deep Sea Research Part I: Oceanographic Research Papers, 97, 67-79, https://doi.org/10.1016/j.dsr.2014.11.015, 2015.

Morales, C., Rogov, M., Wierzbowski, H., Ershova, V., Suan, G., Adatte, T., Föllmi, K. B., Tegelaar, E., Reichart, G.-J., de Lange, G. J., Middelburg, J. J., and van de Schootbrugge, B.: Glendonites track methane seepage in Mesozoic polar seas, Geology, 45, 503-506, 10.1130/g38967.1, 2017.

Müller, R. D., Cannon, J., Qin, X., Watson, R. J., Gurnis, M., Williams, S., Pfaffelmoser, T., Seton, M., Russell, S. H. J., and Zahirovic, S.: GPlates: Building a Virtual Earth Through Deep Time, Geochemistry, Geophysics, Geosystems, 19, 2243-2261, 10.1029/2018gc007584, 2018

Naafs, B. D. A., Inglis, G. N., Zheng, Y., Amesbury, M. J., Biester, H., Bindler, R., Blewett, J., Burrows, M. A., del Castillo Torres, D., Chambers, F. M., Cohen, A. D., Evershed, R. P., Feakins, S. J., Gałka, M., Gallego-Sala, A., Gandois, L., Gray, D. M., Hatcher, P. G., Honorio Coronado, E. N., Hughes, P. D. M., Huguet, A., Könönen, M., Laggoun-Défarge, F., Lähteenoja, O., Lamentowicz, M., Marchant, R., McClymont, E., Pontevedra-Pombal, X., Ponton, C., Pourmand, A., Rizzuti, A. M., Rochefort, L., Schellekens, J., De Vleeschouwer, F., and Pancost, R. D.: Introducing global peat-specific temperature and pH calibrations based on brGDGT bacterial lipids, Geochim Cosmochim Ac, 208, 285-301, https://doi.org/10.1016/j.gca.2017.01.038, 2017.

Naafs, B. D. A., McCormick, D., Inglis, G. N., and Pancost, R. D.: Archaeal and bacterial H-GDGTs are abundant in peat and their relative abundance is positively

Deleted: Krishnan, S., Pagani, M., Huber, M., and Sluijs, A.: High latitude hydrological changes during the Eocene Thermal Maximum 2, Earth and Planetary Science Letters, 404, 167-177, 2014.

correlated with temperature, Geochim Cosmochim Ac, 227, 156-170, https://doi.org/10.1016/j.gca.2018.02.025, 2018a.

Naafs, B. D. A., Rohrssen, M., Inglis, G. N., Lähteenoja, O., Feakins, S. J., Collinson, M. E., Kennedy, E. M., Singh, P. K., Singh, M. P., Lunt, D. J., and Pancost, R. D.: High temperatures in the terrestrial mid-latitudes during the early Palaeogene, Nature Geoscience, 11, 766-771, 10.1038/s41561-018-0199-0, 2018b.

O'Brien, C. L., Robinson, S. A., Pancost, R. D., Sinninghe Damsté, J. S., Schouten, S., Lunt, D. J., Alsenz, H., Bornemann, A., Bottini, C., Brassell, S. C., Farnsworth, A., Forster, A., Huber, B. T., Inglis, G. N., Jenkyns, H. C., Linnert, C., Littler, K., Markwick, P., McAnena, A., Mutterlose, J., Naafs, B. D. A., Püttmann, W., Sluijs, A., van Helmond, N. A. G. M., Vellekoop, J., Wagner, T., and Wrobel, N. E.: Cretaceous sea-surface temperature evolution: Constraints from TEX86 and planktonic foraminiferal oxygen isotopes, Earth-Science Reviews, 172, 224-247, https://doi.org/10.1016/j.earscirev.2017.07.012, 2017.

O'Regan, M., Moran, K., Sangiorgi, F., Brinkhuis, H., Backman, J., Jakobsson, M., Stickley, C. E., Koc, N., Brumsack, H., Willard, D., Pockalny, R., and Skelton, A.: Mid-Cenozoic Tectonic and Paleoenvironmental setting of the Central Arctic Ocean, Paleoceanography, 23, PA1S20, doi:10.1029/2007PA001559, 2008.

Pagani, M., Pedentchouk, N., Huber, M., Sluijs, A., Schouten, S., Brinkhuis, H., Sinninghe Damsté, J. S., Dickens, G. R., and Expedition 302 Scientists, T.: Arctic hydrology during global warming at the Palaeocene-Eocene thermal maximum, Nature, 442, 671-675, 2006.

Park, E., Hefter, J., Fischer, G., Iversen, M. H., Ramondenc, S., Nöthig, E. M., and Mollenhauer, G.: Seasonality of archaeal lipid flux and GDGT-based thermometry in sinking particles of high-latitude oceans: Fram Strait (79°N) and Antarctic Polar Front (50°S), Biogeosciences, 16, 2247-2268, 10.5194/bg-16-2247-2019, 2019.

Pierrehumbert, R. T.: The hydrologic cycle in deep-time climate problems, Nature, 419, 191-198, 2002.

Pitcher, A., Hopmans, E. C., Mosier, A. C., Park, S.-J., Rhee, S.-K., Francis, C. A., Schouten, S., and Sinninghe Damsté, J. S.: Core and Intact Polar Glycerol Dibiphytanyl Glycerol Tetraether Lipids of Ammonia-Oxidizing Archaea Enriched from Marine and Estuarine Sediments, Applied and Environmental Microbiology, 77, 3468-3477, 10.1128/aem.02758-10, 2011a.

Pitcher, A., Wuchter, C., Siedenberg, K., Schouten, S., and Sinninghe Damsté, J. S.: Crenarchaeol tracks winter blooms of ammonia-oxidizing Thaumarchaeota in the coastal North Sea, Limnol Oceanogr, 56, 2308-2318, 10.4319/lo.2011.56.6.2308, 2011b.

Qin, W., Amin, S. A., Martens-Habbena, W., Walker, C. B., Urakawa, H., Devol, A. H., Ingalls, A. E., Moffett, J. W., Armbrust, E. V., and Stahl, D. A.: Marine ammonia-oxidizing archaeal isolates display obligate mixotrophy and wide ecotypic variation, Proceedings of the National Academy of Sciences, 111, 12504-12509, 10.1073/pnas.1324115111, 2014.

Qin, W., Carlson, L. T., Armbrust, E. V., Devol, A. H., Moffett, J. W., Stahl, D. A., and Ingalls, A. E.: Confounding effects of oxygen and temperature on the TEX_{86} signature of marine Thaumarchaeota, Proceedings of the National Academy of Sciences, 112, 10979-10984, 10.1073/pnas.1501568112, 2015.

Reichgelt, T., West, C. K., and Greenwood, D. R.: The relation between global palm distribution and climate, Scientific Reports, 8, 4721, 10.1038/s41598-018-23147-2, 2018.

Richey, J. N., and Tierney, J. E.: GDGT and alkenone flux in the northern Gulf of Mexico: Implications for the TEX86 and UK'37 paleothermometers, Paleoceanography, 31, 1547-1561, 10.1002/2016pa003032, 2016.

Sangiorgi, F., van Soelen, E. E., Spofforth, D. J. A., Pälike, H., Stickley, C. E., St. John, K., Koç, N., Schouten, S., Sinninghe Damsté, J. S., and Brinkhuis, H.: Cyclicity in the middle Eocene central Arctic Ocean sediment record: Orbital forcing and environmental response, Paleoceanography, 23, n/a-n/a, 10.1029/2007PA001487, 2008.

Schouten, S., Hopmans, E. C., Schefuß, E., and Sinninghe Damsté, J. S.: Distributional variations in marine crenarchaeotal membrane lipids: a new tool for reconstructing ancient sea water temperatures?, Earth and Planetary Science Letters, 204, 265-274, 2002.

Schouten, S., Hopmans, E. C., Forster, A., Breugel, Y. V., Kuypers, M. M. M., and Sinninghe Damsté, J. S.: Extremely high sea-surface temperatures at low latitudes during the middle Cretaceous as revealed by archaeal membrane lipids, Geology, 31, 1069-1072, 2003.

Schouten, S., Forster, A., Panoto, F. E., and Sinninghe Damste, J. S.: Towards calibration of the TEX86 palaeothermometer for tropical sea surface temperatures in ancient greenhouse worlds, Org Geochem, 38, 1537-1546, 2007a.

Schouten, S., Baas, M., Hopmans, E. C., and Sinninghe Damsté, J. S.: An unusual isoprenoid tetraether lipid in marine and lacustrine sediments, Org Geochem, 39, 1033-1038, 2008.

Deleted: Schouten, S., Woltering, M., Rijpstra, W. I. C., Sluijs, A., Brinkhuis, H., and Sinninghe Damsté, J. S.: The Paleocene-Eocene carbon isotope excursion in higher plant organic matter: Differential fractionation of angiosperms and conifers in the Arctic, Earth and Planetary Science Letters, 258, 581-592, 2007b.¶

Schouten, S., Hopmans, E. C., Meer, J. v. d., Mets, A., Bard, E., Bianchi, T. S., Diefendorf, A., Escala, M., Freeman, K. H., Furukawa, Y., Ingalls, C. H. a. A., Ménot-Combes, G., Nederbragt, A. J., Oba, M., Pearson, A., Pearson, E. J., Rosell-Melé, A., Schaeffer, P., Shah, S. R., Shanahan, T. M., Smith, R. W., Smittenberg, R., Talbot, H. M., Uchida, M., Mooy, B. A. S. V., Yamamoto, M., Zhang, Z., and Sinninghe Damsté, J. S.: An interlaboratory study of TEX86 and BIT analysis using high-performance liquid chromatography–mass spectrometry, Geochemistry Geophysics Geosystems, 10, Q03012, doi:03010.01029/02008GC002221, 2009.

Schouten, S., Hopmans, E. C., and Sinninghe Damsté, J. S.: The organic geochemistry of glycerol dialkyl glycerol tetraether lipids: A review, Org Geochem, 54, 19-61, http://dx.doi.org/10.1016/j.orggeochem.2012.09.006, 2013.

Schweitzer, H.-J.: Environment and climate in the early Tertiary of Spitsbergen, Palaeogeography, Palaeoclimatology, Palaeoecology, 30, 297-311, 1980.

Seton, M., Müller, R. D., Zahirovic, S., Gaina, C., Torsvik, T., Shephard, G., Talsma, A., Gurnis, M., Turner, M., Maus, S., and Chandler, M.: Global continental and ocean basin reconstructions since 200Ma, Earth-Science Reviews, 113, 212-270, https://doi.org/10.1016/j.earscirev.2012.03.002, 2012.

Shah, S. R., Mollenhauer, G., Ohkouchi, N., Eglinton, T. I., and Pearson, A.: Origins of archaeal tetraether lipids in sediments: Insights from radiocarbon analysis, Geochim Cosmochim Ac, 72, 4577-4594, https://doi.org/10.1016/j.gca.2008.06.021, 2008.

Sinninghe Damsté, J. S., Wakeham, S. G., Kohnen, M. E. L., Hayes, J. M., and de Leeuw, J. W.: A 6,000-year sedimentary molecular record of chemocline excursions in the Black Sea, Nature, 362, 827 - 829, 1993.

Sinninghe Damsté, J. S., Rijpstra, W. I. C., Hopmans, E. C., Weijers, J. W. H., Foesel, B. U., Overmann, J., and Dedysh, S. N.: 13,16-Dimethyl Octacosanedioic Acid (*iso*-Diabolic Acid), a Common Membrane-Spanning Lipid of Acidobacteria

Subdivisions 1 and 3, Applied and Environmental Microbiology, 77, 4147-4154, 10.1128/aem.00466-11, 2011.

Sinninghe Damsté, J. S.: Spatial heterogeneity of sources of branched tetraethers in shelf systems: The geochemistry of tetraethers in the Berau River delta (Kalimantan, Indonesia), Geochim Cosmochim Ac, 186, 13-31, https://doi.org/10.1016/j.gca.2016.04.033, 2016.

Sinninghe Damsté, J. S., Rijpstra, W. I. C., Foesel, B. U., Huber, K. J., Overmann, J., Nakagawa, S., Kim, J. J., Dunfield, P. F., Dedysh, S. N., and Villanueva, L.: An overview of the occurrence of ether- and ester-linked iso-diabolic acid membrane lipids in microbial cultures of the Acidobacteria: Implications for brGDGT paleoproxies for temperature and pH, Org Geochem, 124, 63-76, https://doi.org/10.1016/j.orggeochem.2018.07.006, 2018a.

Sinninghe Damsté, J. S., Rijpstra, W. I. C., Hopmans, E. C., den Uijl, M. J., Weijers, J. W. H., and Schouten, S.: The enigmatic structure of the crenarchaeol isomer, Org Geochem, 124, 22-28, https://doi.org/10.1016/j.orggeochem.2018.06.005, 2018b

Sluijs, A., Schouten, S., Pagani, M., Woltering, M., Brinkhuis, H., Sinninghe Damsté, J. S., Dickens, G. R., Huber, M., Reichart, G.-J., Stein, R., Matthiessen, J., Lourens, L. J., Pedentchouk, N., Backman, J., Moran, K., and The Expedition 302 Scientists: Subtropical Arctic Ocean temperatures during the Palaeocene/Eocene thermal maximum, Nature, 441, 610-613, 2006.

Sluijs, A., Brinkhuis, H., Crouch, E. M., John, C. M., Handley, L., Munsterman, D., Bohaty, S., M., Zachos, J. C., Reichart, G.-J., Schouten, S., Pancost, R. D., Sinninghe Damsté, J. S., Welters, N. L. D., Lotter, A. F., and Dickens, G. R.: Eustatic variations during the Paleocene-Eocene greenhouse world, Paleoceanography, 23, PA4216, doi:10.1029/2008PA001615, 2008a.

Sluijs, A., Röhl, U., Schouten, S., Brumsack, H.-J., Sangiorgi, F., Sinninghe Damsté, J. S., and Brinkhuis, H.: Arctic late Paleocene–early Eocene paleoenvironments with special emphasis on the Paleocene-Eocene thermal maximum (Lomonosov Ridge, Integrated Ocean Drilling Program Expedition 302), Paleoceanography, 23, PA1S11, doi:10.1029/2007PA001495, 2008b.

Sluijs, A., Schouten, S., Donders, T. H., Schoon, P. L., Röhl, U., Reichart, G. J., Sangiorgi, F., Kim, J.-H., Sinninghe Damsté, J. S., and Brinkhuis, H.: Warm and Wet Conditions in the Arctic Region during Eocene Thermal Maximum 2, Nature Geoscience, 2, 777-780, 2009.

Sluijs, A., and Dickens, G. R.: Assessing offsets between the δ13C of sedimentary components and the global exogenic carbon pool across Early Paleogene carbon cycle perturbations, Global Biogeochemical Cycles, 26, GB4005, doi:10.1029/2011GB004224, 2012.

Sollich, M., Yoshinaga, M. Y., Häusler, S., Price, R. E., Hinrichs, K.-U., and Bühring, S. I.: Heat Stress Dictates Microbial Lipid Composition along a Thermal Gradient in Marine Sediments, Frontiers in Microbiology, 8, 10.3389/fmicb.2017.01550, 2017.

Spielhagen, R. F., and Tripati, A.: Evidence from Svalbard for near-freezing temperatures and climate oscillations in the Arctic during the Paleocene and Eocene, Palaeogeography, Palaeoclimatology, Palaeoecology, 278, 48-56, https://doi.org/10.1016/j.palaeo.2009.04.012, 2009.

Stein, R., Boucsein, B., and Meyer, H.: Anoxia and high primary production in the Paleogene central Arctic Ocean: First detailed records from Lomonosov Ridge, Geophysical Research Letters, 33, L18606, doi:10.1029/2006GL026776, 2006.

Deleted: Speelman, E. N., Van Kempen, M. M. L., Barke, J., Brinkhuis, H., Reichart, G. J., Smolders, A. J. P., Roelofs, J. G. M., Sangiorgi, F., De Leeuw, J. W., Lotter, A. F., and Sinninghe Damsté, J. S.: The Eocene Arctic Azolla bloom: environmental conditions, productivity and carbon drawdown, Geobiology, 7, 155-170, 10.1111/j.1472-4669.2009.00195.x, 2009.

Speelman, E. N., Sewall, J. O., Noone, D., Huber, M., der Heydt, A. v., Damsté, J. S., and Reichart, G.-J.: Modeling the influence of a reduced equator-to-pole sea surface temperature gradient on the distribution of water isotopes in the Early/Middle Eocene, Earth and Planetary Science Letters, 298, 57-65, https://doi.org/10.1016/j.epsl.2010.07.026, 2010.

Stein, R.: Upper Cretaceous/lower Tertiary black shales near the North Pole: Organic-carbon origin and source-rock potential, Marine and Petroleum Geology, 24, 67-73, 2007.

Suan, G., Popescu, S.-M., Yoon, D., Baudin, F., Suc, J.-P., Schnyder, J., Labrousse, L., Fauquette, S., Piepjohn, K., and Sobolev, N. N.: Subtropical climate conditions and mangrove growth in Arctic Siberia during the early Eocene, Geology, 45, 539-542, 10.1130/g38547.1, 2017.

Taylor, K. W. R., Huber, M., Hollis, C. J., Hernandez-Sanchez, M. T., and Pancost, R. D.: Re-evaluating modern and Palaeogene GDGT distributions: Implications for SST reconstructions, Global and Planetary Change, 108, 158-174, http://dx.doi.org/10.1016/j.gloplacha.2013.06.011, 2013.

Teichert, B. M. A., and Luppold, F. W.: Glendonites from an Early Jurassic methane seep — Climate or methane indicators?, Palaeogeography, Palaeoclimatology, Palaeoecology, 390, 81-93, https://doi.org/10.1016/j.palaeo.2013.03.001, 2013.

Tierney, J. E., and Tingley, M. P.: A Bayesian, spatially-varying calibration model for the TEX86 proxy, Geochim Cosmochim Ac, 127, 83-106, http://dx.doi.org/10.1016/j.gca.2013.11.026, 2014.

Tierney, J. E., Sinninghe Damsté, J. S., Pancost, R. D., Sluijs, A., and Zachos, J. C.: Eocene temperature gradients, Nature Geosci, 10, 538-539, 10.1038/ngeo2997, 2017.

Torsvik, T. H., Van der Voo, R., Preeden, U., Mac Niocaill, C., Steinberger, B., Doubrovine, P. V., van Hinsbergen, D. J. J., Domeier, M., Gaina, C., Tohver, E., Meert, J. G., McCausland, P. J. A., and Cocks, L. R. M.: Phanerozoic polar wander, palaeogeography and dynamics, Earth-Science Reviews, 114, 325-368, https://doi.org/10.1016/j.earscirev.2012.06.007, 2012.

Trommer, G., Siccha, M., van der Meer, M. T. J., Schouten, S., Sinninghe Damsté, J. S., Schulz, H., Hemleben, C., and Kucera, M.: Distribution of Crenarchaeota tetraether membrane lipids in surface sediments from the Red Sea, Org Geochem, 40, 724-731, https://doi.org/10.1016/j.orggeochem.2009.03.001, 2009.

Uhl, D., Traiser, C., Griesser, U., and Denk, T.: Fossil leaves as palaeoclimate proxies in the Palaeogene of Spitsbergen (Svalbard), Acta Palaeobotanica, 47, 89-107, 2007.

Van der Burgh, J.: Some palms in the Miocene of the lower Rhenish Plain, Review of Palaeobotany and Palynology, 40, 359-374, 1984.

Van Hinsbergen, D. J. J., de Groot, L. V., van Schaik, S. J., Spakman, W., Bijl, P. K., Sluijs, A., Langereis, C. G., and Brinkhuis, H.: A Paleolatitude Calculator for Paleoclimate Studies, PLOS ONE, 10, e0126946, 10.1371/journal.pone.0126946, 2015.

Wakeham, S. G., Amann, R., Freeman, K. H., Hopmans, E. C., Jörgensen, B. B., Putnam, I. F., Schouten, S., Sinninghe Damsté, J. S., Talbot, H. M., and Woebken, D.: Microbial ecology of the stratified water column of the Black Sea as revealed by a comprehensive biomarker stud, Org Geochem, 38, 2070-2097, 2007.

Weijers, J. W. H., Schouten, S., Spaargaren, O. C., and Sinninghe Damsté, J. S.: Occurrence and distribution of tetraether membrane lipids in soils: Implications for the use of the TEX86 proxy and the BIT index, Org Geochem, 37, 1680-1693, 2006.

Weijers, J. W. H., Schouten, S., Sluijs, A., Brinkhuis, H., and Sinninghe Damsté, J. S.: Warm arctic continents during the Palaeocene-Eocene thermal maximum, Earth and Planetary Science Letters, 261, 230-238, 2007a.

Deleted: e

Deleted: Waddell, L. M., and Moore, T. C.: Salinity of the Eocene Arctic Ocean from Oxygen Isotope Analysis of Fish Bone Carbonate, Paleoceanography, 23, PA1S12, doi:10.1029/2007PA001451, 2008.

Deleted: È

Weijers, J. W. H., Schouten, S., van den Donker, J. C., Hopmans, E. C., and Sinninghe Damsté, J. S.: Environmental controls on bacterial tetraether membrane lipid distribution in soils, Geochim Cosmochim Ac, 71, 703-713, 2007b.

Weijers, J. W. H., Lim, K. L. H., Aquilina, A., Sinninghe Damsté, J. S., and Pancost, R. D.: Biogeochemical controls on glycerol dialkyl glycerol tetraether lipid distributions in sediments characterized by diffusive methane flux, Geochemistry, Geophysics, Geosystems, 12, doi:10.1029/2011GC003724, 2011.

Willard, D. A., Donders, T. H., Reichgelt, T., Greenwood, D. R., Sangiorgi, F., Peterse, F., Nierop, K. G. J., Frieling, J., Schouten, S., and Sluijs, A.: Arctic vegetation, temperature, and hydrology during Early Eocene transient global warming events, Global and Planetary Change, 178, 139-152, https://doi.org/10.1016/j.gloplacha.2019.04.012, 2019.

Deleted: Weller, P., and Stein, R.: Paleogene biomarker records from the central Arctic Ocean (Integrated Ocean Drilling Program Expedition 302): Organic carbon sources, anoxia, and sea surface temperature, Paleoceanography, 23, doi:10.1029/2007PA001472, 2008.

Wuchter, C., Schouten, S., Coolen, M. J. L., and Sinninghe Damsté, J. S.: Temperature-dependent variation in the distribution of tetraether membrane lipids of marine Crenarchaeota: Implications for TEX86 paleothermometry, Paleoceanography, 19, PA402, 2004.

Wuchter, C., Schouten, S., Wakeham, S. G., and Sinninghe Damste, J. S.: Temporal and spatial variation in tetraether membrane lipids of marine Crenarchaeota in particulate organic matter: Implications for TEX86 paleothermometry, Paleoceanography, 20, doi:10.1029/2004PA001110, 2005.

Wuchter, C., Abbas, B., Coolen, M. J. L., Herfort, L., van Bleijswijk, J., Timmers, P., Strous, M., Teira, E., Herndl, G. J., Middelburg, J. J., Schouten, S., and Damste, J. S. S.: Archaeal nitrification in the ocean, Proceedings of the National Academy of Sciences of the United States of America, 103, 12317-12322, 10.1073/pnas.0600756103, 2006a.

Wuchter, C., Schouten, S., Wakeham, S. G., and Sinninghe Damsté, J. S.: Archaeal tetraether membrane lipid fluxes in the northeastern Pacific and the Arabian Sea: Implications for TEX86 paleothermometry, Paleoceanography, 21, PA4208, 2006b.

Xie, S., Liu, X.-L., Schubotz, F., Wakeham, S. G., and Hinrichs, K.-U.: Distribution of glycerol ether lipids in the oxygen minimum zone of the Eastern Tropical North Pacific Ocean, Org Geochem, 71, 60-71, https://doi.org/10.1016/j.orggeochem.2014.04.006, 2014.

Yamamoto, M., Shimamoto, A., Fukuhara, T., Tanaka, Y., and Ishizaka, J.: Glycerol dialkyl glycerol tetraethers and TEX86 index in sinking particles in the western North Pacific, Org Geochem, 53, 52-62, https://doi.org/10.1016/j.orggeochem.2012.04.010, 2012.

Zeng, Z., Liu, X.-L., Farley, K. R., Wei, J. H., Metcalf, W. W., Summons, R. E., and Welander, P. V.: GDGT cyclization proteins identify the dominant archaeal sources of tetraether lipids in the ocean, Proceedings of the National Academy of Sciences, 116, 22505-22511, 10.1073/pnas.1909306116, 2019.

Zhang, Y. G., Zhang, C. L., Liu, X.-L., Li, L., Hinrichs, K.-U., and Noakes, J. E.: Methane Index: A tetraether archaeal lipid biomarker indicator for detecting the instability of marine gas hydrates, Earth and Planetary Science Letters, 307, 525-534, https://doi.org/10.1016/j.epsl.2011.05.031, 2011.

Zhang, Y. G., Pagani, M., and Wang, Z.: Ring Index: A new strategy to evaluate the integrity of TEX86 paleothermometry, Paleoceanography, 31, 220-232, doi:10.1002/2015PA002848, 2016.

Zhang, Y. G., and Liu, X.: Export Depth of the TEX86 Signal, Paleoceanography and Paleoclimatology, 33, 666-671, 10.1029/2018pa003337, 2018.

Zhu, J., Poulsen, C. J., and Tierney, J. E.: Simulation of Eocene extreme warmth and high climate sensitivity through cloud feedbacks, Science Advances, 5, eaax1874, 10.1126/sciadv.aax1874, 2019.

Deleted: Zhu, G. Y., Chen, J., Liu, J., Brunzelle, J. S., Huang, B., Wakeham, N., Terzyan, S., Li, X. M., Rao, Z., Li, G. P., and Zhang, X. J. C.: Structure of the APPL1 BAR-PH domain and characterization of its interaction with Rab5, Embo J, 26, 3484-3493, 2007.¶

Figure 1. Location of ACEX Hole 4A within a paleogeographic reconstruction of the Arctic region at the time of the PETM. Reconstruction made using gplates (Müller et al., 2018), with the tectonic reconstruction of Seton et al. (2012, red shape is Lomonosov Ridge in this reconstruction and grey lines are structural features including spreading ridges), the paleomagnetic reference frame of Torsvik et al., (2012), and modern coastlines.

Deleted: using

Deleted: using

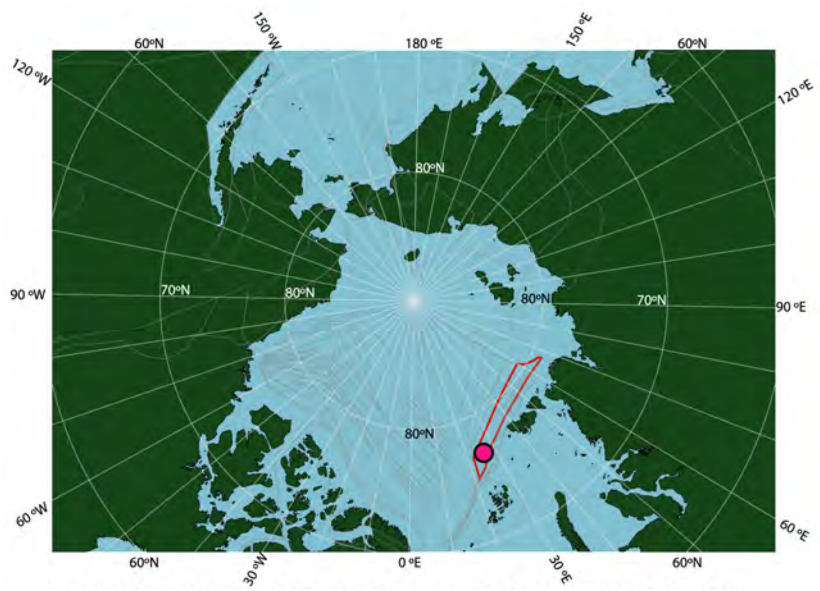

Figure 2. Molecular structures of the relevant isoGDGTs, brGDGTs and brGMGTs and their terminology as described in this study. Crenarchaeol isomer (not shown) differs from Crenarchaeol in the stereochemistry of the cyclopentane moiety adjacent to the cyclohexyl moiety (Sinninghe Damsté et al., 2018b). For the terminology of the brGMGTs, for which the exact chemical structure is still unclear, we follow Baxter et al. (2019), since we identify the same isomers (see Figure S2 for a chromatogram).

Deleted: Chemical

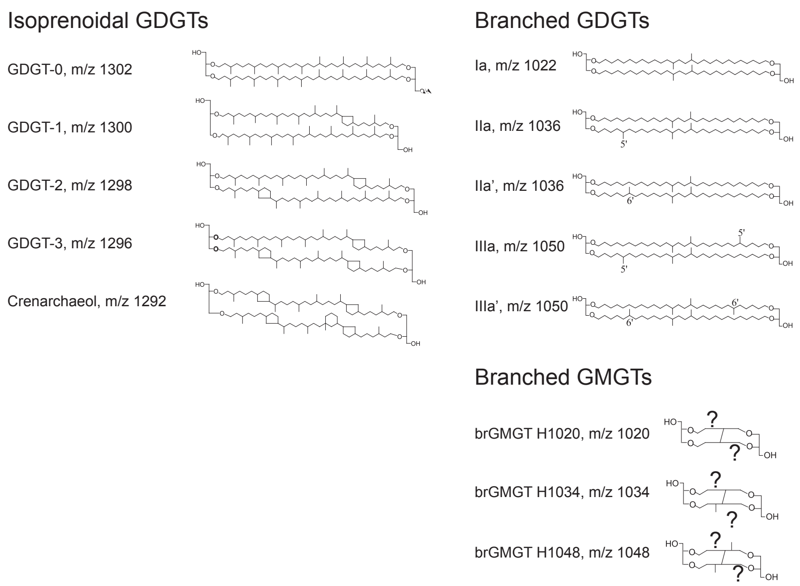

Figure 3. Comparison of the original GDGT dataset of the upper Paleocene and lower Eocene of ACEX Hole 4A (Sluijs et al., 2006; Sluijs et al., 2009) and the new data generated according to the latest chromatography protocols.

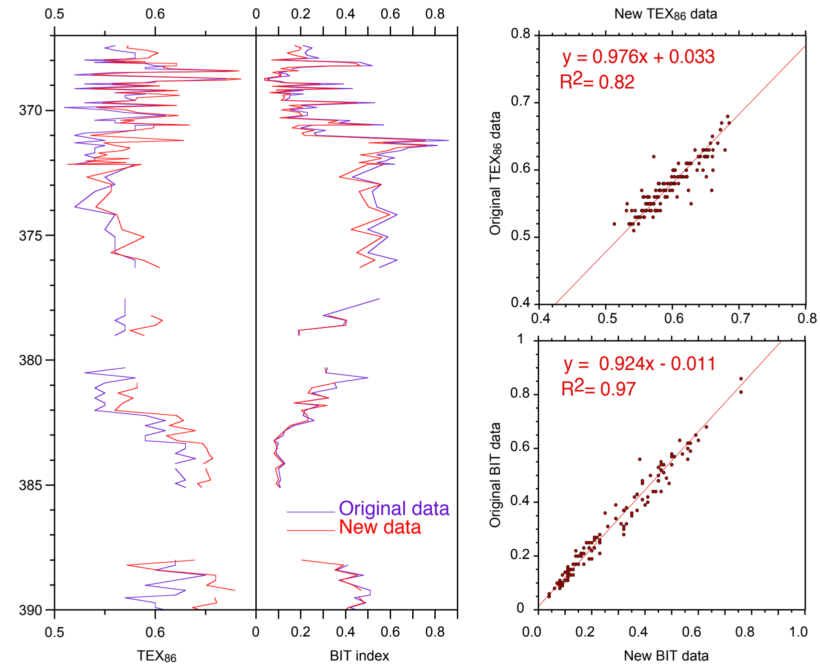

Figure 4. Comparison between BIT index values and TEX_{86} for various intervals spanning the upper Paleocene and lower Eocene of ACEX Hole 4A.

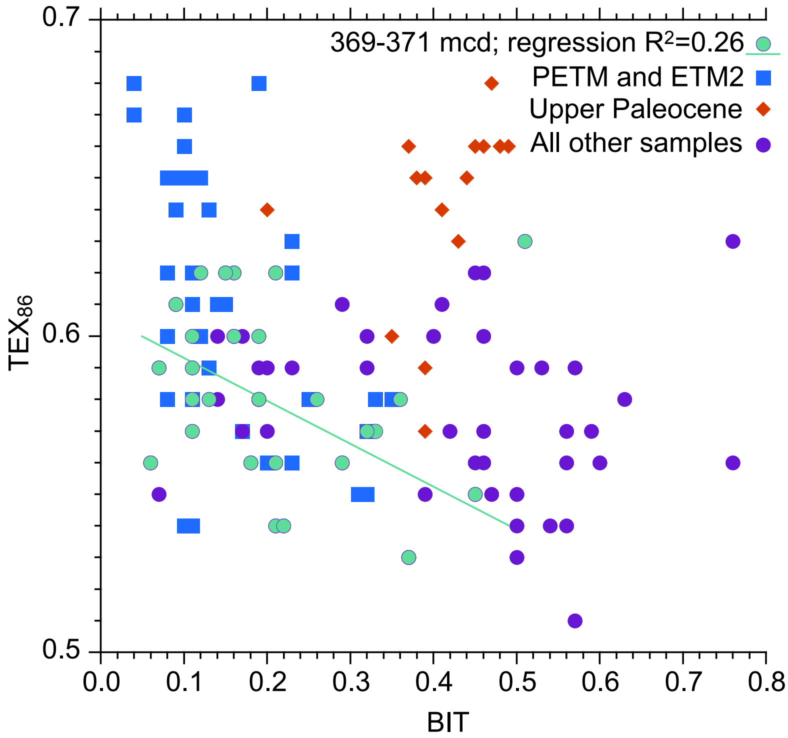

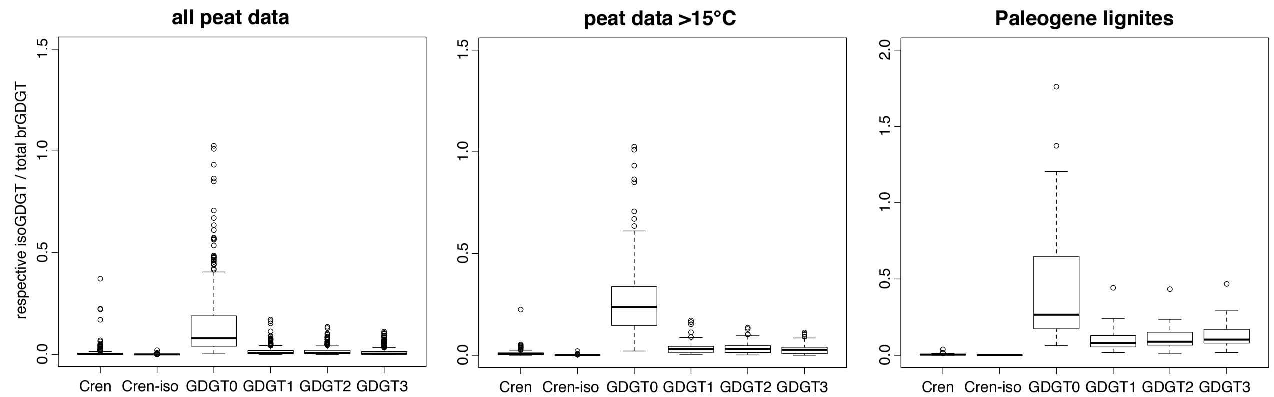

Figure 5. The abundance of various isoGDGTs relative to the total brGDGT abundance in modern peats (left 2 panels) and Paleogene lignites (right panel; Equation 9), used to assess potential isoGDGT contributions to the ACEX samples. The box is standard 25%-50%-75% quantiles, whiskers represent box limits plus/minus 1.5 x the interquartile range (IQR). Any data outside that range is given as circles. Number of measurements per dataset: Modern peats = 473 (most isoGDGTs have been identified in ±430 of those; Modern peats above 15ºC = 141 (all except one of there have isoGDGT data; Lignites = 58 (allof which have isoGDGT data but only 29 have available (quantifiable) crenarchaeol isomer data).

Deleted: s

Deleted: distribution

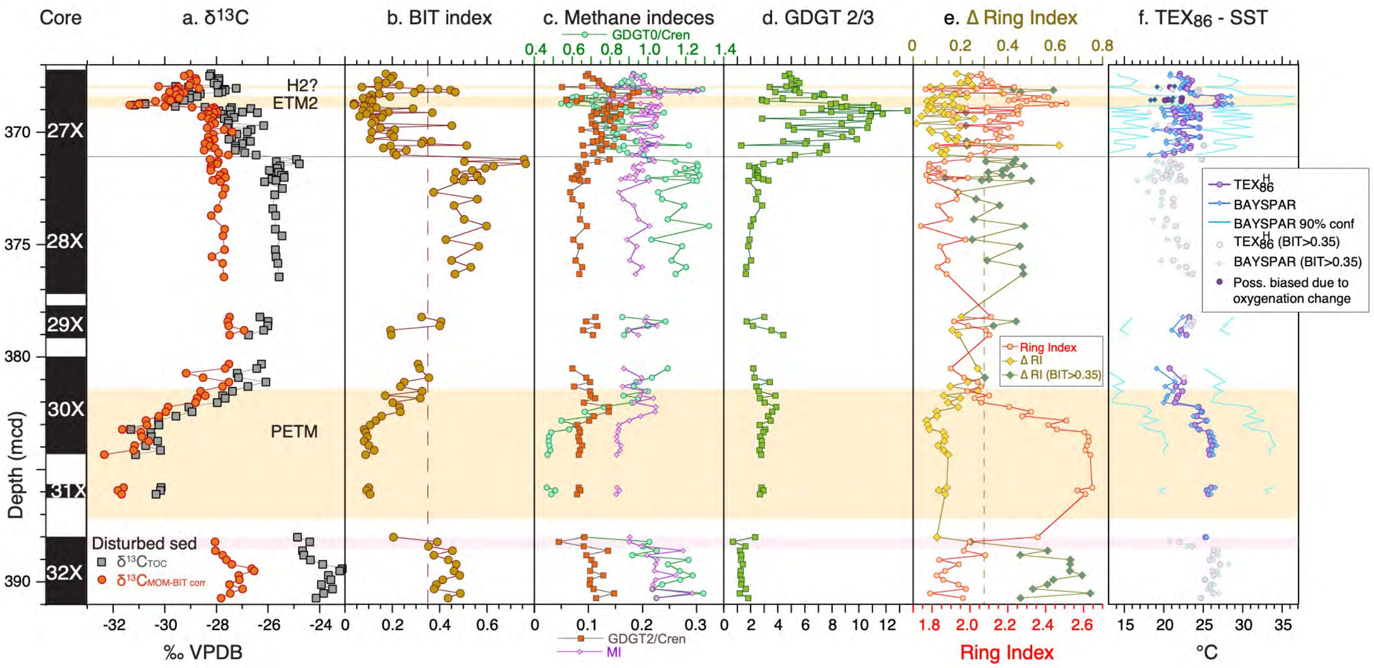

Figure 6. Branched and Isoprenoid GDGT records across the upper Paleocene and lower Eocene of ACEX Hole 4A. a. carbon isotope stratigraphy (total organic carbon record from Sluijs et al., 2006 and 2009; marine organic matter record from Sluijs and Dickens (2012)), b. BIT index (equation 2), c. indices indicative of anaerobic archaeal methanotrophy (MI index (equation 3) and GDGT-2/Crenarchaeol), and methanogenesis (GDGT-0/Crenarchaeol), d. GDGT2-GDGT3 ratio, e. Ring index (equation 5) and Δ Ring Index, f. TEX_{86} (equation 1) calibrated to sea surface temperature using a non-linear calibration TEX_{86}^{H} calibration (Kim et al., 2010) and the BAYSPAR method, which is based on a linear calibration (Tierney and Tingley, 2014).

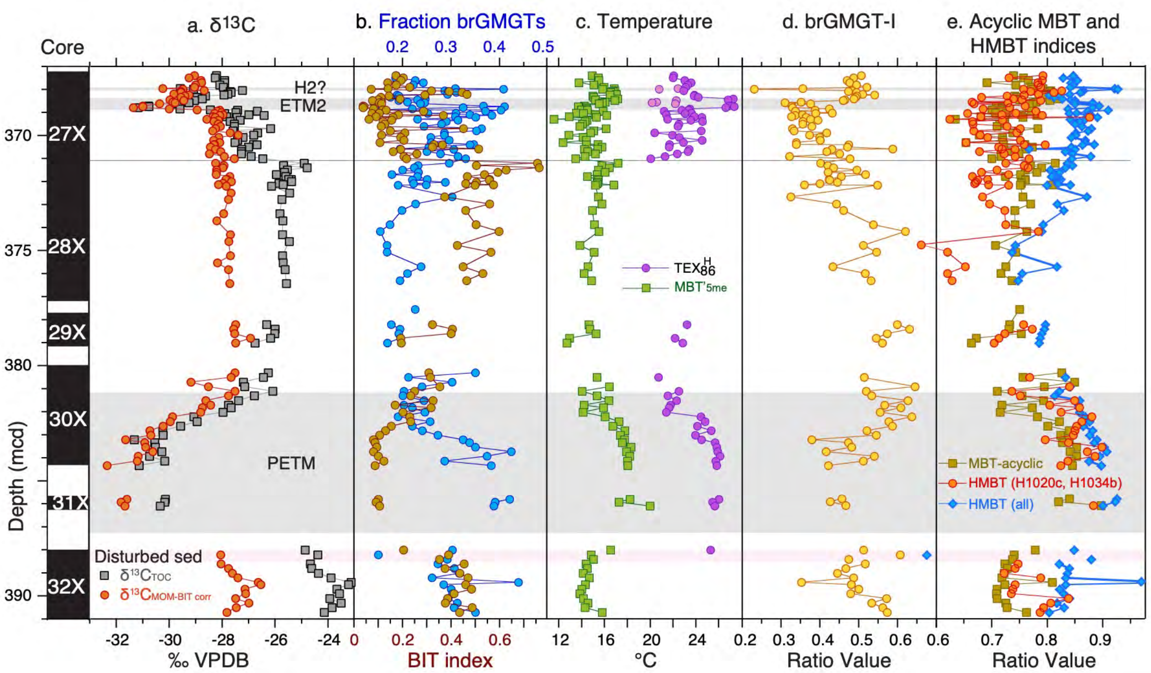

Figure 7. Branched GMGT records across the upper Paleocene and lower Eocene of ACEX Hole 4A. a. carbon isotope stratigraphy (total organic carbon record from Sluijs et al., 2006 and 2009; marine organic matter record from Sluijs and Dickens (2012)), b. fraction of brGMGTs of the total branched GDGTs and GMGTs and BIT index (equation 2), c. MBT'_{5me} record (Willard et al., 2019) and TEX_{86}^{H}, d. MBT*acyclic* (equation 6) and H-MBT based on all isomers detected with m/z 1020 and m/z 1034 (H-MBT all; equation 7) and based on H1020a and H1034b (H-MBT H1020a, H1034c), e. brGMGT-1 record (equation 8).

Page 2: [1] Deleted	Appy Sluijs1	28/04/2020 16:49:00

Page 2: [2] Deleted	Appy Sluijs1	28/04/2020 16:54:00

Page 2: [3] Deleted	Appy Sluijs1	28/04/2020 17:02:00

Page 2: [4] Deleted	Appy Sluijs1	28/04/2020 17:02:00